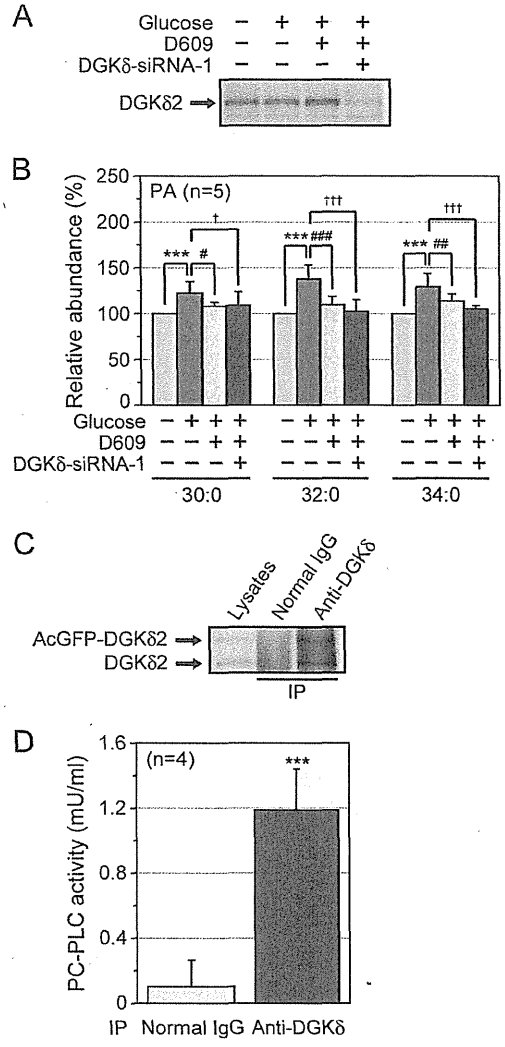

FIGURE 8. **Examination of the functional linkage between PC-PLC and DGKδ.** Effects of D609 and DGKδ-siRNA-1 on high glucose-induced increases of PA molecular species in C2C12 myoblasts were compared. *A*, the suppression of DGKδ2 expression by DGKδ-siRNA-1 was confirmed by Western blot analysis using the anti-DGKδ antibody. *B*, 30:0-, 32:0-, and 34:0-PA in the glucose-unstimulated or glucose-stimulated cells treated with DMSO (control), D609, or D609 and DGKδ-siRNA-1 were detected using the LC/ESI-MS method. The results are presented as the percentage of the value of PA molecular species in glucose-unstimulated cells. The values are presented as the mean ± S.D. ($n = 5$). ***, $p < 0.005$ (no stimulation *versus* glucose stimulation). #, $p < 0.05$; ##, $p < 0.01$; ###, $p < 0.005$ (without D609 *versus* with D609). †, $p < 0.05$; †††, $p < 0.005$ (control siRNA *versus* DGKδ-siRNA-1). *C* and *D*, co-immunoprecipitation of PC-PLC activity with DGKδ2. *C*, immunoprecipitation (*IP*) of DGKδ2 using the anti-DGKδ antibody was confirmed by Western blot analysis using the anti-DGKδ antibody. *D*, PC-PLC activity in the precipitates was measured using the Amplex Red® PC-PLC assay kit. The values are presented as the mean ± S.D. ($n = 4$). ***, $p < 0.005$. When the assay was performed in the absence of alkaline phosphatase, the activity was not detectable.

taining arachidonic acid (*e.g.* 38:4 (18:0/20:4)-DG) derived from PI turnover (7, 19, 20). However, high glucose stimulation did not increase the amount of 38:4-PA (Figs. 1 and 2), which mainly consisted of 18:0/20:4-PA (Table 1). Moreover, DGKδ-siRNAs and DGKδ2 overexpression failed to affect the amounts of 38:4-PA in response to high glucose stimulation (Figs. 2 and 4). These results indicate that DGKδ does not phosphorylate 38:4-DG derived from PI turnover in a glucose-dependent manner.

DGKδ did not exhibit selectivity against 16:0/16:0 (32:0)- or 16:0/18:1 (34:1)-DG *in vitro* (Fig. 5). Therefore, we hypothesized that DGKδ exerts substrate selectivity in C2C12 cells through accessing a DG pool containing 30:0-, 32:0-, and 34:0-DG, and not via its intrinsic preference. There are three DG supply pathways, *i.e.* 1) *de novo* synthesis including acetyl-CoA carboxylase (30, 31), 2) the PLD/PA phosphatase route (32), and 3) PC hydrolysis by PC-specific PLC (33). Treatment with the PC-PLC inhibitor D609, but not inhibitors of acetyl-CoA carboxylase and PLD, strongly inhibited the high glucose stimulation-responsive production of 30:0-, 32:0-, and 34:0-PA (Fig. 7*A*). Moreover, RNA silencing of DGKδ failed to further inhibit the glucose-dependent increases in 30:0-, 32:0-, and 34:0-PA in the presence of D609 (Fig. 8*B*). Furthermore, PC-PLC was co-immunoprecipitated with DGKδ2 (Fig. 8*D*). Taken together, these results strongly suggest that 30:0-, 32:0-, and 34:0-DG phosphorylated by DGKδ2 in response to acute high glucose exposure are generated, at least in part, by PC hydrolysis catalyzed by PC-PLC (Fig. 9).

The role of sphingomyelin synthase as a potential PC-PLC was indicated (36). We cannot rule out the possibility that DGKδ2 partly utilizes sphingomyelin synthase-dependent DG. However, it is likely that DGKδ2 phosphorylates DG species generated, at least in part, by PC-PLC because the co-immunoprecipitates with DGKδ2 contained PC-PLC activity.

The molecular identity of PC-PLC remains unclear (35). In this study, DGKδ was revealed to directly or indirectly associate with PC-PLC. With the pulldown of PC-PLC activity with DGKδ2, there may be an opportunity to identify the unidentified PC-PLC enzyme by proteomics approaches. Therefore, DGKδ2 may serve as a good tool to search for the PC-PLC molecule.

D609 attenuated high glucose-dependent increases in various C30-C34 DG species (Fig. 7*C*). However, D609 strongly inhibited only the high glucose stimulation-responsive production of 30:0-, 32:0-, and 34:0-PA (Fig. 7*A*). Intriguingly, this inhibitor statistically reduced the amounts of 30:0-, 32:0-, and 34:0-DG in the absence of high glucose (Fig. 7*B*). Therefore, it is likely that, in response to acute high glucose stimulation (5 min), DGKδ2 mainly utilizes these DG species supplied from the PC-PLC pathway in a high glucose-independent manner. Moreover, DGKδ2 can generate 30:1-, 32:1-, and 34:1-PA, in addition to 30:0-, 32:0-, and 34:0-PA. (Figs. 2 and 4). Although D609 moderately attenuated 30:1-, 32:1-, and 34:1-PA generation (Fig. 7*A*), this inhibitor did not affect the amounts of 30:1-, 32:1-, and 34:1-DG in the absence of high glucose stimulation (Fig. 7*B*). However, D609 substantially inhibited high glucose-dependent increases for 30:1-, 32:1-, and 34:1-DG (Fig. 7*C*). These results suggest that DGKδ2 can utilize 30:1-, 32:1-, and 34:1-DG that are supplied from the PC-PLC pathway in a high glucose-dependent manner.

Recently, Shulga *et al.* (37) and Lowe *et al.* (38) reported that DGKδ positively regulated lipid synthesis, including DG and PA, during adipocyte differentiation. However, unlike for acute high glucose stimulation, a significant preference against DG and PA was not found. The increases were, at least in part, a

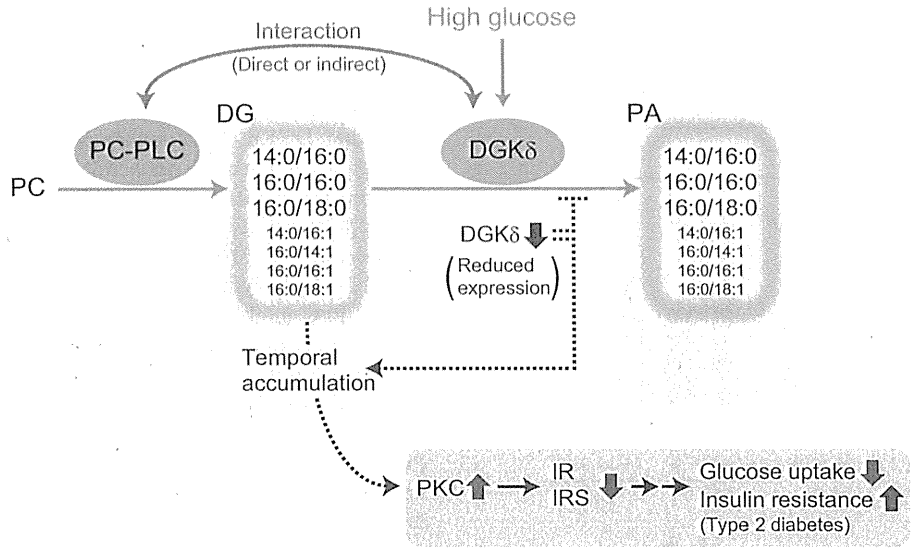

FIGURE 9. **Model for the metabolism pathway utilized by DGKδ.** *IR*, insulin receptor; *IRS*, insulin receptor substrate.

result of promoting the *de novo* synthesis of fatty acids. However, in this study, an inhibitor of acetyl-CoA carboxylase TOFA did not decrease glucose-stimulated PA production (Fig. 6*A*). Because differentiation is a long term event, the difference between acute high glucose stimulation in C2C12 myoblasts and adipocyte differentiation may be due to distinct supply pathways and/or fatty acid conversion during long term culture through the remodeling pathway (Lands' cycle) (39).

Chibalin *et al.* (15) previously reported that the transcription of DGKδ and the levels of DGKδ protein were also reduced in skeletal muscle from type II diabetes patients. Moreover, in DGKδ haploinsufficient mice ($DGK\delta^{+/-}$), the accumulation of DG, which was caused by decreases in total DGK activity and DGKδ protein levels in skeletal muscle, increased phosphorylation of PKCδ and suppressed protein expression of the insulin receptor and insulin receptor substrate-1 for insulin signaling, resulting in the aggravation of type II diabetes (15). Another study reported that the accumulation of DG molecular species with palmitic acid (16:0) is involved in insulin resistance (40). It is generally accepted that saturated fatty acids including palmitic acid induce insulin resistance (41–43). In this study, MS/MS analysis demonstrated that 30:0-, 30:1-, 32:0-, 32:1-, 34:0-, and 34:1-PA commonly contained palmitic acid (16:0), and suggests that DGKδ mainly consumes 30:0-, 30:1-, 32:0-, 32:1-, 34:0-, and 34:1-DG containing palmitic acid (16:0) supplied from the PC-PLC pathway for glucose uptake in skeletal muscle in a glucose-dependent manner. Acute high glucose- and DGKδ-dependent increases in 30:0-, 30:1-, 32:0-, 32:1-, 34:0-, and 34:1-PA were relatively minor changes (20–30% increases) when compared with the total amounts of each PA species (Figs. 1 and 2). DGKδ, which was temporarily activated within 5 min (16), showed a distinct punctate localization pattern in C2C12 cells (17). Therefore, a possible explanation of these findings is that these DGKδ-dependent minor changes of DG/PA species in temporally and spatially restricted regions play a role in modulating insulin signaling. However, further studies are required to elucidate the relationship between the specific DG species accumulation in type II diabetes patients and the PC-PLC-DGKδ pathway disclosed here.

In summary, the present study strongly suggests that DGKδ preferentially consumes palmitic acid (16:0)-containing DG species such as 30:0-, 30:1-, 32:0-, 32:1-, 34:0-, and 34:1-DG, but not arachidonic acid (20:4)-containing DG species derived from the phosphatidylinositol turnover, in glucose-stimulated C2C12 myoblasts (Fig. 9). Moreover, an unexpected linkage between PC-PLC and DGKδ emerged. The route "PC → PC-PLC → DG → DGK → PA" proposed here (Fig. 9) is a novel DG metabolic pathway. This new pathway is proposed to play an important role in glucose uptake in skeletal muscle and to be involved in the pathogenesis of type 2 diabetes.

REFERENCES

1. Zimmet, P., Alberti, K. G., and Shaw, J. (2001) Global and societal implications of the diabetes epidemic. *Nature* **414,** 782–787
2. Biddinger, S. B., and Kahn, C. R. (2006) From mice to men: insights into the insulin resistance syndromes. *Annu. Rev. Physiol.* **68,** 123–158
3. Kraegen, E. W., Saha, A. K., Preston, E., Wilks, D., Hoy, A. J., Cooney, G. J., and Ruderman, N. B. (2006) Increased malonyl-CoA and diacylglycerol content and reduced AMPK activity accompany insulin resistance induced by glucose infusion in muscle and liver of rats. *Am. J. Physiol. Endocrinol. Metab.* **290,** E471–E479
4. Goto, K., Hozumi, Y., and Kondo, H. (2006) Diacylglycerol, phosphatidic acid, and the converting enzyme, diacylglycerol kinase, in the nucleus. *Biochim. Biophys. Acta* **1761,** 535–541
5. Mérida, I., Avila-Flores, A., and Merino, E. (2008) Diacylglycerol kinases: at the hub of cell signalling. *Biochem. J.* **409,** 1–18
6. Sakane, F., Imai, S., Kai, M., Yasuda, S., and Kanoh, H. (2007) Diacylglycerol kinases: why so many of them? *Biochim. Biophys. Acta* **1771,** 793–806
7. Shulga, Y. V., Topham, M. K., and Epand, R. M. (2011) Regulation and functions of diacylglycerol kinases. *Chem. Rev.* **111,** 6186–6208
8. van Blitterswijk, W. J., and Houssa, B. (2000) Properties and functions of diacylglycerol kinases. *Cell. Signal.* **12,** 595–605
9. Sakai, H., and Sakane, F. (2012) Recent progress on type II diacylglycerol kinases: the physiological functions of diacylglycerol kinase δ, η and κ and their involvement in disease. *J. Biochem.* **152,** 397–406
10. Sakane, F., Imai, S., Kai, M., Yasuda, S., and Kanoh, H. (2008) Diacylglycerol kinases as emerging potential drug targets for a variety of diseases. *Curr. Drug Targets* **9,** 626–640

11. Sakane, F., Imai, S., Yamada, K., Murakami, T., Tsushima, S., and Kanoh, H. (2002) Alternative splicing of the human diacylglycerol kinase δ gene generates two isoforms differing in their expression patterns and in regulatory functions. *J. Biol. Chem.* **277,** 43519–43526
12. Murakami, T., Sakane, F., Imai, S., Houkin, K., and Kanoh, H. (2003) Identification and characterization of two splice variants of human diacylglycerol kinase η. *J. Biol. Chem.* **278,** 34364–34372
13. Sakane, F., Imai, S., Kai, M., Wada, I., and Kanoh, H. (1996) Molecular cloning of a novel diacylglycerol kinase isozyme with a pleckstrin homology domain and a C-terminal tail similar to those of the EPH family of protein tyrosine kinase. *J. Biol. Chem.* **271,** 8394–8401
14. DeFronzo, R. A., Jacot, E., Jequier, E., Maeder, E., Wahren, J., and Felber, J. P. (1981) The effect of insulin on the disposal of intravenous glucose: results from indirect calorimetry and hepatic and femoral venous catheterization. *Diabetes* **30,** 1000–1007
15. Chibalin, A. V., Leng, Y., Vieira, E., Krook, A., Björnholm, M., Long, Y. C., Kotova, O., Zhong, Z., Sakane, F., Steiler, T., Nylén, C., Wang, J., Laakso, M., Topham, M. K., Gilbert, M., Wallberg-Henriksson, H., and Zierath, J. R. (2008) Downregulation of diacylglycerol kinase δ contributes to hyperglycemia-induced insulin resistance. *Cell* **132,** 375–386
16. Miele, C., Paturzo, F., Teperino, R., Sakane, F., Fiory, F., Oriente, F., Ungaro, P., Valentino, R., Beguinot, F., and Formisano, P. (2007) Glucose regulates diacylglycerol intracellular levels and protein kinase C activity by modulating diacylglycerol-kinase subcellular localization. *J. Biol. Chem.* **282,** 31835–31843
17. Takeuchi, M., Sakiyama, S., Usuki, T., Sakai, H., and Sakane, F. (2012) Diacylglycerol kinase δ1 transiently translocates to the plasma membrane in response to high glucose. *Biochim. Biophys. Acta* **1823,** 2210–2216
18. Hodgkin, M. N., Pettitt, T. R., Martin, A., Michell, R. H., Pemberton, A. J., and Wakelam, M. J. (1998) Diacylglycerols and phosphatidates: which molecular species are intracellular messengers? *Trends Biochem. Sci.* **23,** 200–204
19. Rodriguez de Turco, E. B., Tang, W., Topham, M. K., Sakane, F., Marcheselli, V. L., Chen, C., Taketomi, A., Prescott, S. M., and Bazan, N. G. (2001) Diacylglycerol kinase ϵ regulates seizure susceptibility and long-term potentiation through arachidonoyl-inositol lipid signaling. *Proc. Natl. Acad. Sci. U.S.A.* **98,** 4740–4745
20. Tang, W., Bunting, M., Zimmerman, G. A., McIntyre, T. M., and Prescott, S. M. (1996) Molecular cloning of a novel human diacylglycerol kinase highly selective for arachidonate-containing substrates. *J. Biol. Chem.* **271,** 10237–10241
21. Mizuno, S., Sakai, H., Saito, M., Kado, S., and Sakane, F. (2012) Diacylglycerol kinase-dependent formation of phosphatidic acid molecular species during interleukin-2 activation in CTLL-2 T-lymphocytes. *FEBS Open Bio.* **2,** 267–272
22. Amtmann, E. (1996) The antiviral, antitumoural xanthate D609 is a competitive inhibitor of phosphatidylcholine-specific phospholipase C. *Drugs Exp. Clin. Res.* **22,** 287–294
23. Halvorson, D. L., and McCune, S. A. (1984) Inhibition of fatty acid synthesis in isolated adipocytes by 5-(tetradecyloxy)-2-furoic acid. *Lipids* **19,** 851–856
24. Pizer, E. S., Thupari, J., Han, W. F., Pinn, M. L., Chrest, F. J., Frehywot, G. L., Townsend, C. A., and Kuhajda, F. P. (2000) Malonyl-coenzyme-A is a potential mediator of cytotoxicity induced by fatty-acid synthase inhibition in human breast cancer cells and xenografts. *Cancer Res.* **60,** 213–218
25. Su, W., Yeku, O., Olepu, S., Genna, A., Park, J. S., Ren, H., Du, G., Gelb, M. H., Morris, A. J., and Frohman, M. A. (2009) 5-Fluoro-2-indolyl deschlorohalopemide (FIPI), a phospholipase D pharmacological inhibitor that alters cell spreading and inhibits chemotaxis. *Mol. Pharmacol.* **75,** 437–446
26. Bligh, E. G., and Dyer, W. J. (1959) A rapid method of total lipid extraction and purification. *Can. J. Biochem. Physiol.* **37,** 911–917
27. Sakai, H., Tanaka, Y., Tanaka, M., Ban, N., Yamada, K., Matsumura, Y., Watanabe, D., Sasaki, M., Kita, T., and Inagaki, N. (2007) ABCA2 deficiency results in abnormal sphingolipid metabolism in mouse brain. *J. Biol. Chem.* **282,** 19692–19699
28. Callender, H. L., Forrester, J. S., Ivanova, P., Preininger, A., Milne, S., and Brown, H. A. (2007) Quantification of diacylglycerol species from cellular extracts by electrospray ionization mass spectrometry using a linear regression algorithm. *Anal. Chem.* **79,** 263–272
29. Imai, S., Yasuda, S., Kai, M., Kanoh, H., and Sakane, F. (2009) Diacylglycerol kinase δ associates with receptor for activated C kinase 1, RACK1. *Biochim. Biophys. Acta* **1791,** 246–253
30. Craven, P. A., Davidson, C. M., and DeRubertis, F. R. (1990) Increase in diacylglycerol mass in isolated glomeruli by glucose from de novo synthesis of glycerolipids. *Diabetes* **39,** 667–674
31. Wolf, B. A., Easom, R. A., McDaniel, M. L., and Turk, J. (1990) Diacylglycerol synthesis *de novo* from glucose by pancreatic islets isolated from rats and humans. *J. Clin. Invest.* **85,** 482–490
32. Bandyopadhyay, G., Sajan, M. P., Kanoh, Y., Standaert, M. L., Quon, M. J., Reed, B. C., Dikic, I., and Farese, R. V. (2001) Glucose activates protein kinase C-ζ/λ through proline-rich tyrosine kinase-2, extracellular signal-regulated kinase, and phospholipase D: a novel mechanism for activating glucose transporter translocation. *J. Biol. Chem.* **276,** 35537–35545
33. Ramana, K. V., Friedrich, B., Tammali, R., West, M. B., Bhatnagar, A., and Srivastava, S. K. (2005) Requirement of aldose reductase for the hyperglycemic activation of protein kinase C and formation of diacylglycerol in vascular smooth muscle cells. *Diabetes* **54,** 818–829
34. Schütze, S., Berkovic, D., Tomsing, O., Unger, C., and Krönke, M. (1991) Tumor necrosis factor induces rapid production of 1′2′diacylglycerol by a phosphatidylcholine-specific phospholipase C. *J. Exp. Med.* **174,** 975–988
35. Adibhatla, R. M., Hatcher, J. F., and Gusain, A. (2012) Tricyclodecan-9-yl-xanthogenate (D609) mechanism of actions: a mini-review of literature. *Neurochem. Res.* **37,** 671–679
36. Luberto, C., and Hannun, Y. A. (1998) Sphingomyelin synthase, a potential regulator of intracellular levels of ceramide and diacylglycerol during SV40 transformation: Does sphingomyelin synthase account for the putative phosphatidylcholine-specific phospholipase C? *J. Biol. Chem.* **273,** 14550–14559
37. Shulga, Y. V., Loukov, D., Ivanova, P. T., Milne, S. B., Myers, D. S., Hatch, G. M., Umeh, G., Jalan, D., Fullerton, M. D., Steinberg, G. R., Topham, M. K., Brown, H. A., and Epand, R. M. (2013) Diacylglycerol kinase δ promotes lipogenesis. *Biochemistry* **52,** 7766–7776
38. Lowe, C. E., Zhang, Q., Dennis, R. J., Aubry, E. M., O'Rahilly, S., Wakelam, M. J., and Rochford, J. J. (2013) Knockdown of diacylglycerol kinase δ inhibits adipocyte differentiation and alters lipid synthesis. *Obesity* **21,** 1823–1829
39. Shindou, H., Hishikawa, D., Harayama, T., Yuki, K., and Shimizu, T. (2009) Recent progress on acyl CoA:lysophospholipid acyltransferase research. *J. Lipid Res.* **50,** (suppl.) S46–S51
40. Coll, T., Eyre, E., Rodríguez-Calvo, R., Palomer, X., Sánchez, R. M., Merlos, M., Laguna, J. C., and Vázquez-Carrera, M. (2008) Oleate reverses palmitate-induced insulin resistance and inflammation in skeletal muscle cells. *J. Biol. Chem.* **283,** 11107–11116
41. Hu, F. B., van Dam, R. M., and Liu, S. (2001) Diet and risk of Type II diabetes: the role of types of fat and carbohydrate. *Diabetologia* **44,** 805–817
42. Hunnicutt, J. W., Hardy, R. W., Williford, J., and McDonald, J. M. (1994) Saturated fatty acid-induced insulin resistance in rat adipocytes. *Diabetes* **43,** 540–545
43. Vessby, B., Uusitupa, M., Hermansen, K., Riccardi, G., Rivellese, A. A., Tapsell, L. C., Nälsén, C., Berglund, L., Louheranta, A., Rasmussen, B. M., Calvert, G. D., Maffetone, A., Pedersen, E., Gustafsson, I. B., Storlien, L. H., and KANWU Study (2001) Substituting dietary saturated for monounsaturated fat impairs insulin sensitivity in healthy men and women: the KANWU Study. *Diabetologia* **44,** 312–319

Carcinogenesis vol.35 no.2 pp.272–281, 2014
doi:10.1093/carcin/bgt343
Advance Access publication October 15, 2013

Heat shock factor 1 accelerates hepatocellular carcinoma development by activating nuclear factor-κB/mitogen-activated protein kinase

Makoto Chuma*, Naoya Sakamoto, Akira Nakai[1], Shuhei Hige, Mitsuru Nakanishi, Mitsuteru Natsuizaka, Goki Suda, Takuya Sho, Kanako Hatanaka[2], Yoshihiro Matsuno[2], Hideki Yokoo[3], Toshiya Kamiyama[3], Akinobu Taketomi[3], Gen Fujii[4], Kosuke Tashiro[5], Yoko Hikiba[6], Mitsuaki Fujimoto[1], Masahiro Asaka and Shin Maeda[7]

Department of Gastroenterology and Hepatology, Hokkaido University, Kita 15, Nishi 7, Kita-ku, Sapporo 060-8638, Japan, [1]Department of Biochemistry and Molecular Biology, Yamaguchi University, Ube, Japan, [2]Department of Pathology and [3]Department of Gastroenterological Surgery I, Hokkaido University, Kita 15, Nishi 7, Kita-ku, Sapporo 060-8638, Japan, [4]Division of Cancer Prevention, National Cancer Center Research Institute, Tokyo, Japan, [5]Graduate School of Genetic Resources Technology, Kyushu University, Fukuoka, Japan, [6]Division of Gastroenterology, Institute for Adult Diseases, Asahi Life Foundation, Tokyo, Japan and [7]Department of Gastroenterology, Yokohama City University, Yokohama, Japan

*To whom correspondence should be addressed. Tel: +81 11-716-1611; Fax: +81 11-706-7867;
Email: mchuuma@med.hokudai.ac.jp

Heat shock factor 1 (HSF1), a major transactivator of stress responses, has been implicated in carcinogenesis in various organs. However, little is known about the biological functions of HSF1 in the development of hepatocellular carcinoma (HCC). To clarify the functional role of HSF1 in HCC, we established HSF1-knockdown (HSF1 KD) KYN2 HCC cells by stably expressing either small hairpin RNA (shRNA) against HSF1 (i.e. HSF1 KD) or control shRNA (HSF1 control). Tumorigenicity was significantly reduced in orthotopic mice with HSF1 KD cells compared with those with HSF1 control cells. Reduced tumorigenesis in HSF1 KD cells appeared attributable to increased apoptosis and decreased proliferation. Tumor necrosis factor-α-induced apoptosis was increased in HSF1 KD cells and HSF1$^{-/-}$ mouse hepatocytes compared with controls. Decreased expression of IκB kinase γ, a positive regulator of nuclear factor-κB, was also observed in HSF1 KD cells and HSF1$^{-/-}$ mouse hepatocytes. Furthermore, expression of bcl-2-associated athanogene domain 3 (BAG3) was dramatically reduced in HSF1 KD cells and HSF1$^{-/-}$ mouse hepatocytes. We also found that epidermal growth factor-stimulated mitogen-activated protein kinase signaling was impaired in HSF1 KD cells. Clinicopathological analysis demonstrated frequent overexpression of HSF1 in human HCCs. Significant correlations between HSF1 and BAG3 protein levels and prognosis were also observed. In summary, these results identify a mechanistic link between HSF1 and liver tumorigenesis and may provide as a potential molecular target for the development of anti-HCC therapies.

Introduction

Hepatocellular carcinoma (HCC) is one of the most common malignant tumors and the third leading cause of cancer death worldwide (1). Despite marked advances in diagnostic and therapeutic techniques, prognosis remains unsatisfactory for HCC patients (2,3). An understanding of HCC carcinogenesis at the molecular level is thus urgently needed in order to identify novel molecular targets for the development of more effective therapies.

Heat shock factor 1 (HSF1) is the main regulator of the heat shock response, which is involved in protecting cells and organisms from heat, ischemia, inflammation, oxidative stress and other noxious conditions (4,5). Under various forms of physiological stress, HSF1 drives the production of heat shock proteins (HSPs), such as HSP27, HSP70 and HSP90, which act as protein chaperones (5,6). The functions of HSF1 are not limited to increasing the expression of chaperones; HSF1 also modulates the expression of hundreds of genes other than chaperones that are critical for survival under an array of potentially lethal stressors (6–8). As a result, HSF1 influences fundamental cellular processes such as cell cycle control, protein translation, glucose metabolism and proliferation (7–12). In human tumors, constitutive expression of Hsp27, Hsp70 and Hsp90 at high levels predicts poor prognosis and resistance to therapy (13–15). These effects are often attributable to HSF1-dependent mechanisms (16). Thus, as a master regulator of cellular processes, the roles of HSF1 in carcinogenesis and tumor progression are now emerging. Several recent investigations using mouse models have suggested that HSF1 is involved in carcinogenesis (9,17). In clinical samples, HSF1 is often constitutively expressed at high levels in a variety of tumors, including breast cancer (7,18), pancreatic cancer (19), prostate carcinoma (20) and oral squamous cell carcinoma (21).

Hepatocarcinogenesis is a multistep process, in the majority of cases slowly developing within a well-defined etiology of viral infection and chronic alcohol abuse, leading to the chronic hepatitis and cirrhosis that are regarded as preneoplastic stages (22). A great number of factors, receptors and downstream elements of signaling cascades regulate proliferation and apoptosis. Dysregulation of the balance between cell proliferation and apoptosis thus plays a critical role in hepatocarcinogenesis (23,24). Two of the major pathways of cell proliferation and apoptosis are nuclear factor kappa B (NF-κB) signaling and mitogen-activated protein kinase (MAPK) signaling. NF-κB transcription factors are critical regulators of genes involved in inflammation and the suppression of apoptosis. NF-κB has been shown to be instrumental for tumor promotion in colitis-associated cancer and inflammation-associated liver cancer (25,26). Activation of the extracellular signal-regulated kinase (ERK)/MAPK pathway regulates many important cellular processes, such as proliferation, differentiation, angiogenesis, survival and cell adhesion (27). Importantly, the ERK/MAPK pathway is constitutively activated in HCC (28).

The present study investigated the biological influences of HSF1 in HCC cell proliferation and apoptosis involving the NF-κB and MAPK signal pathways. We found that HSF1 deficiency significantly diminished NF-κB and MAPK activation in primary hepatocytes and HCC cells, so HSF1 deficiency inhibited the development of HCC. Furthermore, clinicopathological analysis demonstrated a significant correlation between HSF1 protein level and prognosis. Our results suggest HSF1 as a promising molecular target for the development of anti-HCC therapeutics.

Abbreviations: BAG3, bcl-2-associated athanogene domain 3; EGFR, epidermal growth factor receptor; ERK, extracellular signal-regulated kinase; FACS, fluorescence-activated cell sorting; HCC, hepatocellular carcinoma; HSF1, heat shock factor 1; HSF1 KD, HSF1 knockdown; HSP, heat shock protein; IKKγ, IκB kinase gamma; LPS, lipopolysaccharide; MAPK, mitogen-activated protein kinase; MEK, mitogen-activated protein kinase kinase; mRNA, messenger RNA; NF-κB, nuclear factor kappa B; PCNA, proliferating cell nuclear antigen; SCID, severe combined immune-deficient mice; shRNA, small hairpin RNA; TNF-α, tumor necrosis factor alpha; TUNEL, terminal deoxynucleotidyl transferase-mediated deoxyuridine triphosphate nick-end labeling; WT, wild type.

Materials and methods

Cell cultures and reagents

Human HCC cell lines HepG2, PLC/PRF/5, HLE and HLF were obtained from the American Type Culture Collection. Huh7 was obtained from the Japanese Collection of Research Bioresources Cell Bank (Ibaraki, Japan). KIM-1 and KYN2 were kindly provided by Dr Hirohisa Yano (Department of Pathology, Kurume University, Kurume, Japan). Li7 was kindly provided by Dr Yae Kanai (Division of Molecular Pathology, National Cancer Center Research Institute,

Tokyo, Japan). HepG2, PLC/PRF/5, Huh7, HLE and HLF cells were maintained in Dulbecco's modified Eagle's medium containing 10% fetal bovine serum. KIM-1 and KYN2 was maintained in RPMI medium containing 10% fetal bovine serum.

Antibodies and chemicals

The antibodies used included: anti-HSF1, ERK1/2, phosphor-ERK1/2, MAPK kinase (MEK), phospho-MEK, phosphor- efficiently activated epidermal growth factor receptor (EGFR), cyclin D1, cdc2, CDK4, phospho-IκBα, IκB kinase gamma (IKKγ), IKKβ, caspase-3 and Bcl-X_L (Cell Signaling Biotechnology, Danvers, MA); anti-HSP90, HSP72, β-actin and proliferating cell nuclear antigen (PCNA) (Santa Cruz Biotechnology, Santa Cruz, CA); anti-EGFR (Millipore, Billerica, MA); anti-HSP70/HSP72 (Enzo Life science, NY); and anti-BAG3 (Abcam, Cambridge, UK).

Biochemical and immunohistochemical analyses

Protein lysates were prepared from tissues and cultured cells, separated by sodium dodecyl sulfate–polyacrylamide gel electrophoresis, transferred onto Immobilon membranes (Millipore) and analyzed by immunoblotting. Total cellular RNA was extracted using Trizol reagent (Invitrogen, Carlsbad, CA), then cDNA was synthesized using SuperScript II (Invitrogen), and expression of specific messenger RNAs (mRNAs) was quantified using real-time PCR and normalized against glyceraldehyde-3-phosphate dehydrogenase mRNA expression. Details of real-time PCR conditions and primer sequences are available in Supplementary Materials and methods, available at *Carcinogenesis* Online. Immunohistochemical staining was performed on formalin-fixed, paraffin-embedded tissue sections using immunoperoxidase methods, as described previously (15). For array analysis, we used the Human WG-6 BeadChip-kit (Illumina, San Diego, CA) in accordance with the instructions from the manufacturer (details are given in Supplementary Materials and methods, available at *Carcinogenesis* Online).

Establishment of HSF1-knockdown cells

A HSF1 small hairpin RNA (shRNA) plasmid and negative control plasmid were purchased from SABiosciences (QIAGEN, Valencia, CA). The shRNA sequences targeting HSF1 were from position 5′-CAGGTTGTTCATAGTCAGAAT-3′ as in the nucleotide sequence of HSF1. As a negative control, a shRNA was designed with the sequence 5′-GGAATCTCATTCGATGCATAC-3′. Transfection was achieved using Oligofectamine reagent (Invitrogen) according to the instructions from the manufacturer. To establish stable knockdown cell lines, shRNA plasmids were transfected into KYN2 cells and cultured in the presence of puromycin (Sigma–Aldrich, St Louis, MO).

Cell proliferation and bromodeoxyuridine assay

Cell proliferation in response to HSF1 silencing was determined by trypan blue exclusion assay. DNA synthesis was determined by bromodeoxyuridine assay according to the instructions from the manufacturer (Roche Diagnostics, Basel, Switzerland). The result was expressed as a percentage of the maximum absorbance at 450 nm, based on three independent experiments. Cells were counted using a Coulter Counter (Beckman Coulter, Pasadena, CA).

Apoptosis assay

Assessment of apoptosis was performed by measuring the intensity of the sub-G_1 peak. For the sub-G_1 peak, HSF1 control KYN2 cells or HSF1-knockdown (HSF1 KD) KYN2 cells were tumor necrosis factor alpha (TNF-α) treatment for 24 h. Cells were treated with propidium iodide and then the sub-G_1 peak was analyzed with a fluorescence-activated cell sorting (FACS) flow cytometer (FACSCalibur; Becton Dickinson, San Jose, CA). Terminal deoxynucleotidyl transferase-mediated deoxyuridine triphosphate nick-end labeling (TUNEL) assay was performed in accordance with the manufacturer's instructions (ApopTag kit; Intergen, Burlington, MA).

Animals

HSF1-deficient ($HSF^{-/-}$) mice have been described previously (29). C57BL/6 wild-type (WT) mice were purchased from CLEA Japan (Tokyo, Japan) for use in the experiments, with primary hepatocytes isolated using a collagenase perfusion method as described in a previous report (26). For orthotopic implantation, C.B-17/Icr-scid/scidJcl [severe combined immune-deficient mice (SCID)] mice were obtained from CLEA Japan. All mice were maintained in filter-topped cages on autoclaved food and water at the University of Hokkaido and the Institute for Adult Diseases, Asahi Life Foundation, according to National Institutes of Health (NIH) guidelines. All experimental protocols were approved by the ethics committee for animal experimentation at Hokkaido University and Asahi Life Foundation. Orthotopic implantation of KYN2 cells and KYN2 transfectants were performed as described previously (30). Briefly, mice were inoculated orthotopically with 5×10^6 HSF1 control ($n = 12$) and HSF1 KD ($n = 12$) cells in 100 μl of phosphate-buffered saline, injected into the liver. Mice were killed 6 weeks after inoculation and autopsies were performed immediately. In the lipopolysaccharide (LPS)/D-galactosamine (GalN)-induced liver injury model, mice were injected intraperitoneally with LPS (20 lg/kg; Sigma) and GalN (1000 mg/kg; Wako, Osaka, Japan) (24).

Patients and tissue samples

For immunohistochemical analysis, a total of 226 adult patients with HCC who underwent curative resection between 1997 and 2006 at Hokkaido University Hospital were enrolled in this study. A preoperative clinical diagnosis of HCC was required to meet the diagnostic criteria of the American Association for the Study of Liver Diseases. Briefly, inclusion criteria were as follows: (i) distinctive pathological diagnosis, (ii) no preoperative anticancer treatment or distant metastases, (iii) curative liver resection (exclusion of extrahepatic tumor spread/metastasis) and (iv) complete clinicopathological and follow-up data. The study protocols were approved by the institutional review board and performed in compliance with the Helsinki of Declaration. Written informed consent was obtained from as many of the patients who were alive as possible (deceased cases were approved for use without written informed consent). Histological diagnosis was made according to World Health Organization criteria. The main clinicopathological features are presented in Table I. During follow-up, clinical evaluations and biochemical tests were performed every 1–3 months. Patients underwent triphasic computed tomography of the liver every 2–3 months.

Statistical analysis

Data are expressed as mean ± standard error of the mean (SEM). Significant differences were detected using non-parametric testing. Correlations between protein expression and clinicopathological features of the specimens were assessed, and the resulting data were analyzed using the χ^2 test and Fisher's exact test. Cumulative survival rate was calculated from the first date of treatment using the Kaplan–Meier life-table method. Differences were evaluated by log-rank testing. Independent factors for survival were assessed with the Cox proportional hazard regression model. Differences between the two groups were analyzed using the log-rank test. Statistical analyses were performed using Stat View software (version 5.0; SAS Institute, Cary, NC). Values of $P < 0.05$ were considered significant.

Results

Effect of HSF1 on tumor growth

We first investigated expression of HSF1 in cultured HCC cell lines. HSF1 expression was detected in all eight HCC cell lines analyzed. KYN2 cells showed significantly higher expression of HSF1 than other cell lines (Figure 1A). To further elucidate the functional role of HSF1 in HCC, we established HSF1 KD KYN2 cells by expressing the shRNA against HSF1 or control shRNA. To evaluate the effects of HSF1 on cell growth, we measured cell numbers at several time points and found that the growth of HSF1 KD cells was significantly inhibited compared with control cells (HSF1 control) (Figure 1B). Cell cycle regulators including PCNA, cyclin D1, cdc2 and CDK4 were suppressed in HSF1 KD cells compared with HSF1 control cells (Figure 1C). These results indicate that HSF1 enhances HCC cell growth. Concordantly, HSF1 KD reduced DNA synthesis as measured by bromodeoxyuridine incorporation (Figure 1D).

To evaluate the effects of HSF1 on HCC *in vivo*, orthotopic xenografts were established by HSF1 control and HSF1 KD KYN2 cells in nude mice. Maximum primary tumor diameters and tumor volumes were significantly decreased in HSF1 KD xenografts compared with HSF1 control ones (Figure 1E), suggesting that HSF1 accelerated HCC tumor growth *in vivo*. We confirmed that the tumor of HSF1 KD cells showed significantly lower expression of HSF1 and PCNA than the tumor of HSF1 control cells (Figure 1E).

We performed gain-of-function experiments for HSF1 *in vitro*. No apparent changes in cell growth were seen with overexpression of HSF1 in HCC cell lines with low HSF1 expression (Supplementary Figure 1, available at *Carcinogenesis* Online), whereas cell growth was reduced in HSF1 KD experiments, as above. Based on these

Table I. HSF1, BAG3 expression and clinicopathological variables in HCC

Parameter	Total	HSF1		*P*	BAG3		*P*
		High	Low		High	Low	
		n = 115	*n* = 111		*n* = 112	*n* = 114	
		≥30	<30		≥25	<25	
Age (years)							
≥60	126	66	60	0.69	59	67	0.42
<60	100	49	51		53	47	
Sex							
Male	185	95	90	0.86	94	91	0.49
Female	41	20	21		18	23	
Etiology							
HBsAg(+)/HCV(−)	85	45	40	0.70	39	46	0.67
HBsAg(−)/HCV(+)	84	43	41		44	40	
HBsAg(+)/HCV(+)	6	4	2		2	4	
HBsAg(−)/HCV(−)	51	23	28		27	24	
Cirrhosis							
Presence	121	64	57	0.59	62	59	0.59
Absence	105	51	54		50	55	
Tumor size (cm)							
<5	149	67	82	0.017*	66	83	0.035*
≥5	77	48	29		46	31	
No. of tumor nodules							
Solitary	168	78	90	0.032*	79	89	0.22
Multiple (≥2)	58	37	21		33	25	
TNM stage							
I and II	139	62	77	0.017*	63	76	0.11
III and IV	87	53	34		49	38	
BCLC stage							
A	81	27	54	<0.001*	32	49	0.065
B	108	64	44		58	50	
C	37	24	13		22	15	
Differentiation							
Well	36	11	25	0.010*	10	26	0.014*
Moderate	143	74	69		75	68	
Poor	47	30	17		27	20	
Capsular formation							
Presence	184	95	89	0.73	91	93	1.0
Absence	42	20	22		21	21	
Vascular invasion							
Present	37	24	13	0.073	22	15	0.21
Absent	189	91	98		90	99	
Serum AFP level							
<20	117	53	64	0.086	52	65	0.14
≥20	109	62	47		60	49	

AFP, alpha-fetoprotein; BCLC, Barcelona Clinic Liver Cancer; HCV, hepatitis C virus; TNM, tumor node metastasis.
*Significant *P* value.

findings, we concluded that HSF1 expression is a necessary condition for cell growth, but it is not a sufficient condition. We, therefore, did not further investigate gain of function of HSF1.

Impaired EGF-mediated MEK/ERK activation in HSF1 KD cells and HSF1$^{-/-}$ hepatocytes

Activation of the MEK/ERK pathway regulates many important cellular processes in carcinogenesis. To further elucidate the function of HSF1 on tumor growth, we investigated the cascade of MAPK. In WT hepatocytes and HSF1 control cells, EGF, a potent activator of MAPK, efficiently activated EGFR, MEK1/2 and ERK1/2 (Figure 2A). In contrast, activation of EGFR, MEK1/2 or ERK1/2 was significantly decreased in HSF-knockout mice (HSF$^{-/-}$) hepatocytes and HSF1 KD cells (Figure 2A and B). Regarding protein levels of EGFR, MEK1/2 and ERK1/2, EGFR protein levels were significantly decreased in HSF1$^{-/-}$ hepatocytes and HSF1 KD compared with controls, whereas other proteins were unchanged (Figure 2A and B). This result was consistent with the previous report (31). Immunohistochemical staining revealed that HSF1 control tumor showed strong phosphorylated ERK1/2 levels, whereas almost no ERK1/2 activation was observed in HSF1 KD tumors (Figure 2C).

Role of HSF1 in TNF-α-induced apoptosis

Since tumor growth inhibition is caused mainly by increased cell death and decreased cellular proliferation, we compared numbers of apoptotic cell deaths in HSF1 control and HSF KD xenografts using the TUNEL assay. Significantly more apoptotic tumor cells were found in HSF1 KD tumors than in HSF1 control tumors (Figure 3A). Next, we examined whether HSF1 was involved in apoptosis *in vitro*. FACS analysis showed very few apoptotic cells in HSF KD or HSF control in the absence of any stimuli. In contrast, treatment with TNF-α, a potent inducer of apoptosis, caused more extensive apoptotic cell death in HSF1 KD cells (23.9%) than in HSF control cells (8.7%) (Figure 3B). Furthermore, we also confirmed increased TNF-α-induced apoptosis in HSF KD cells as determined by TUNEL assay and caspase-3 activation (Figure 3C and D). To examine whether HSF1 is required for TNF-α-induced liver apoptosis *in vivo*, we used an LPS/GalN liver injury model that depends on TNF-α-mediated apoptosis (32). At 7 h LPS/GalN

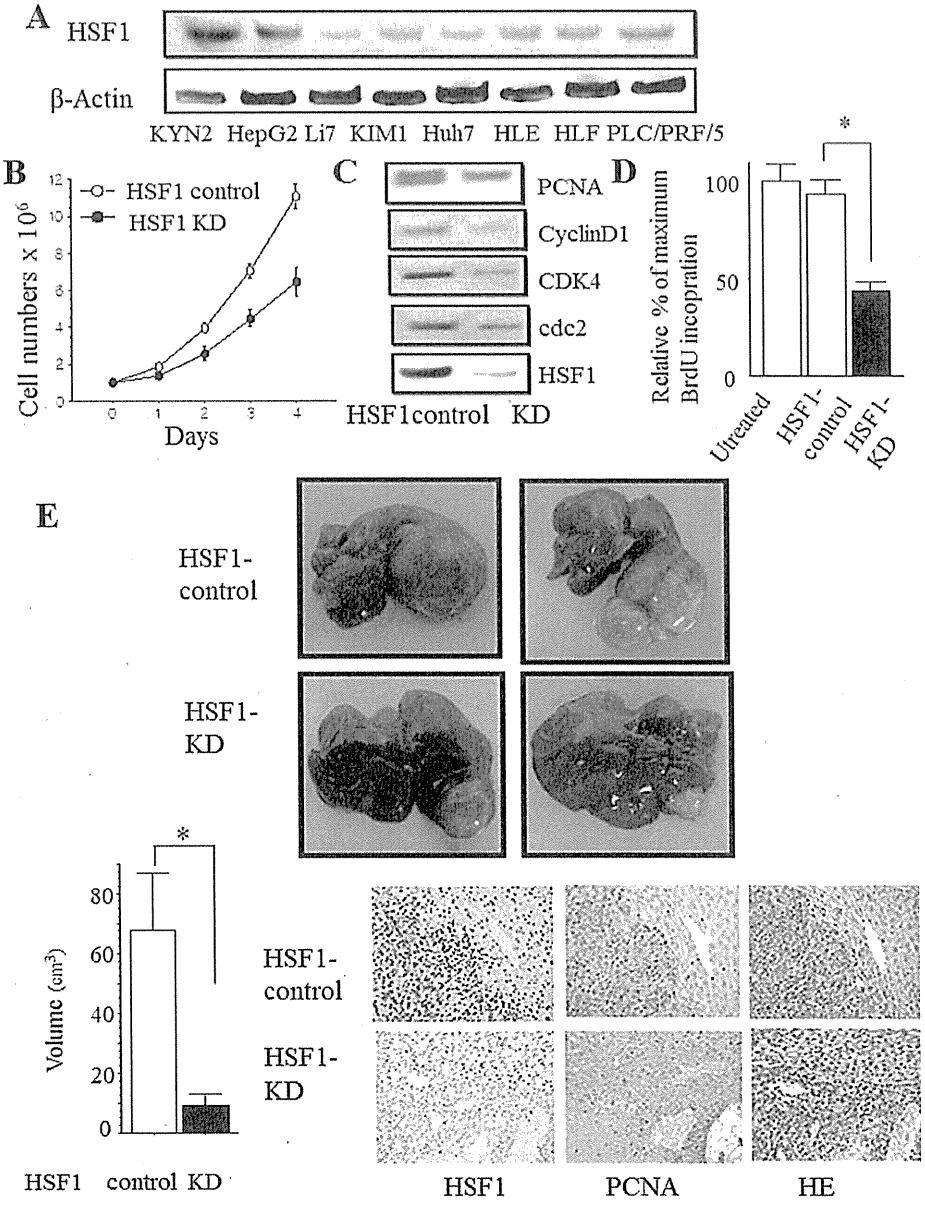

Fig. 1. Role of HSF1 in HCC growth. (**A**) Expression of HSF1 in the eight indicated HCC cell lines was determined by western blot analysis, using β-actin as a control. (**B**) Cell growth of HSF1 control KYN2 cells and HSF1 KD KYN2 cells was measured by counting the number of cells. One representative experiment from three experiments is shown. Data are plotted as mean ± SEM. (**C**) Expression of cell-cycle-related protein in HSF1 control KYN2 cells and HSF1 KD KYN2 cells, as determined by western blot analysis. (**D**) Cells were pulsed with BrdU (10 mmol/l) for 4 h. Optical density values are expressed as a percentage relative to the group expressing control. $^*P < 0.05$. Bars: SEM. (**E**) Growth appearance of HSF1 KD and HSF1 control cells in SCID mice after orthotopic implantation (upper panel). Orthotopic tumor volume was measured. Data are expressed as mean ± SEM (HSF1 control, $n = 12$; HSF1 KD, $n = 12$). $^*P < 0.05$. Bars: SEM (lower left panel). HE and immunohistochemical staining for HSF1 and PCNA (original magnification: ×40): lower right panel. BrdU, bromodeoxyuridine; HE, hematoxylin and eosin.

administration, $HSF^{-/-}$ exhibited marked alanine aminotransferase elevation (Figure 3E), severe histological liver damage and hepatocyte apoptosis compared with WT mice (Figure 3E). This was also in accordance with the notable depression of HSF1 inducing apoptosis *in vitro*.

HSF1 is involved in TNF-α-mediated NF-κB activation

Regarding the association between HSF1 and antiapoptosis, expression of bcl-2-associated athanogene domain 3 (BAG3) was reportedly reduced in HSF1 KD cells compared with control cells (7,11). In addition, microarray array analysis showed that BAG3 was dramatically downregulated in HSF1 KD cells compared with HSF1 control cells (Supplementary Table I, available at *Carcinogenesis* Online). Immunoblot analysis showed that BAG3 protein expression was reduced in $HSF1^{-/-}$ hepatocytes and HSF1 KD cells relative to the respective controls (Figure 4A and B). Meanwhile, activation of IKK and NF-κB pathway represents one of the most important antiapoptotic signals. In addition, BAG3 is also reported to control proteasomal degradation of IKKγ, the regulatory subunit (also called NF-κB essential modulator) of the IKK complex, and

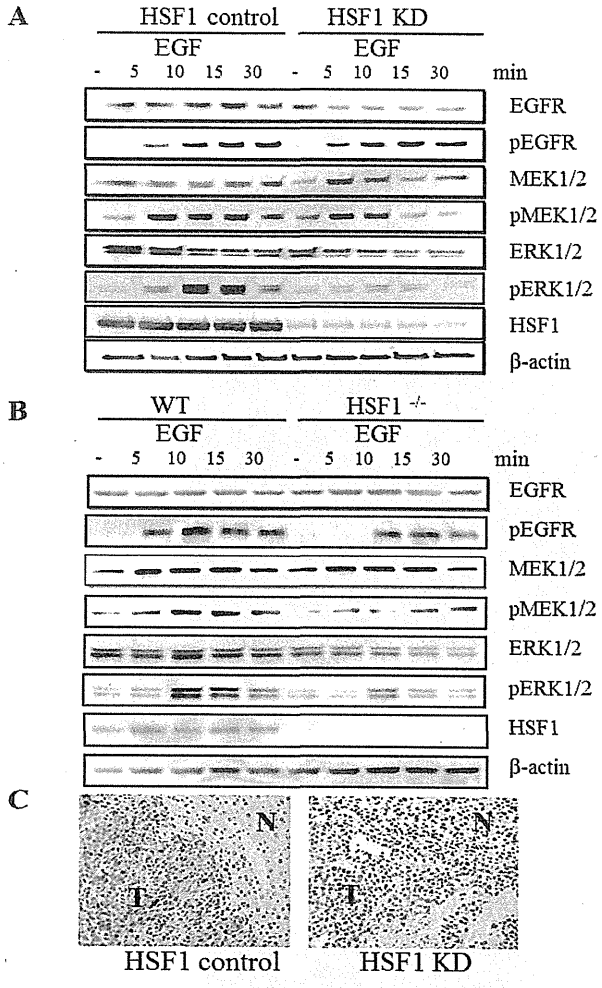

Fig. 2. EGF-mediated MEK/ERK activation is impaired in HSF1 KD cells and HSF1$^{-/-}$ hepatocytes. (**A**) HSF1 control and KD cells were treated with EGF (10 ng/ml), lysed at the indicated times, gel separated and immunoblotted with antibodies against indicated proteins. (**B**) HSF1 WT and HSF$^{-/-}$ hepatocytes were treated with TNF-α (30 ng/ml), lysed in indicated times, gel separated and immunoblotted with antibodies against indicated proteins. (**C**) Representative phosphorylated ERK (p-ERK) staining of orthotopic tumors of HSF1 control and KD cells (original magnification: ×40). N, non-cancerous liver; T, tumor.

NF-κB activity (33). Regarding the NF-κB pathway, NF-κB activation by TNF-α was decreased in HSF1 KD cells compared with the control cells (Figure 4A). In contrast, without any treatment, basal NF-κB activity was very weak and no differences were apparent between HSF1 control cells and HSF1 KD cells (Figure 4A). Consistent with this, microarray analysis showed no apparent differences in the expression of typical NF-κB-regulated genes. We also performed NF-κB pathway analysis and found that the pathway was not overrepresented by the microarray results (Supplementary Figure 2, available at *Carcinogenesis* Online). Next, we investigated whether HSF1 is involved in TNF-α-mediated NF-κB activation and found that phosphorylated Iκk-B (p-IκB), a marker of NF-κB activation, was significantly decreased in HSF$^{-/-}$ hepatocytes and HSF1 KD cells compared with their controls. As expected, IKKγ protein levels were dramatically reduced in HSF1$^{-/-}$ hepatocytes and HSF1 KD cells compared with their controls (Figure 4A and B). To investigate whether decreased IKKγ protein was degraded via proteasome, we used the proteasomal inhibitor, MG-132, and found that protein levels of IKKγ in HSF1 KD cells recovered with the inhibitor, whereas protein expression of BAG3 was unchanged (Figure 4C). Although mRNA levels of BAG3 were significantly downregulated in HSF1 KD cells compared with HSF1 control cells, mRNA levels of IKKγ were not changed (Figure 4D). HSP70 mRNA and protein levels were similar between HSF1 control and HSF1 KD cells (Figure 4A–D). These results suggest that HSF1 positively regulated BAG3 expression, which stabilized the IKKγ protein necessary for NF-κB activation. Immunohistochemical staining revealed that downregulation of HSF1 dramatically reduced BAG3 levels in HSF1 KD xenografts compared with the HSF1 control xenografts.

We performed real-time PCR analysis of the putative NF-κB-regulated antiapoptotic genes. The levels of A20, cellular inhibitor of apoptosis 2 (c-IAP2) RNA expression were decreased in HSF1 KD cells by TNF-α-mediated compared with HSF1 control cells, whereas cylindromatosis, cIAP1 were unchanged (Figure 4E). These results suggest that HSF1 plays an important role in tumor growth via MAPK-mediated cellular proliferation and NF-κB-mediated antiapoptosis.

HSF1 and BAG3 were frequently overexpressed in human HCCs

To analyze the involvement of HSF1 in HCCs, we examined expression levels of HSF1 in human primary HCCs. Immunoblot analysis showed that levels of HSF1 in HCC tissues were significantly higher than in non-cancerous liver tissues in 5 of 10 samples (50%) (Figure 5A). We tested 226 samples from tumor tissues of patients with HCCs by immunohistochemistry. The median percentage of positive cells was 30% (range: 0–90.0%) and we divided patients into two groups of high expressers and low expressers based on the percentage of HSF1-positive cells using a cutoff level of 30%, representing the median value of HSF1. We found that 50.9% (115/226) of tumor samples showed high HSF1 expression. Typical examples of high HSF1 expression samples are shown in Figure 5B. The characteristics of patients in this analysis are shown in Table I. Significant differences were apparent between high and low HSF1 expression groups in terms of tumor size ($P = 0.017$), tumor node metastasis stage ($P = 0.017$), Barcelona Clinic Liver Cancer stage ($P < 0.001$), number of tumor nodules ($P = 0.032$) and histological grade ($P = 0.010$) (Table I), but no significant correlations were observed between HSF1 expression and other clinicopathological variables such as etiology or cirrhosis (Table I). Furthermore, patients with tumors showing HSF1 overexpression displayed significantly shorter overall survival (median: 75.2 months) compared with patients whose tumors showed HSF1 low expression (median: 136.0 months; $P = 0.004$, log-rank test) (Figure 5C). These findings suggest that overexpression of HSF1 was frequently observed in human HCCs, particularly in tumors exhibiting aggressive features.

To explore the pathological relationship between HSF1 and BAG3 in HCC samples, we performed immunohistochemical analysis for BAG3 in 226 HCC samples, which were also analyzed for HSF1 immunohistochemistry. The median percentage of positive cells was 25% (range: 0–85.0%) and we divided them into two groups—high expressers and low expressers—based on the percentage of BAG3-positive cells using a cutoff level of 25%, representing the median value of BAG3. Representative examples of immunohistochemical reactivity for BAG3 are shown in Figure 5B. Expressions of BAG3 protein were significantly increased in HCC specimens, whereas no or only low BAG3 expression was seen in adjacent non-cancerous tissue. BAG3 expression correlated significantly with histological grade ($P = 0.014$), and tumor size ($P = 0.035$), but no significant correlations were observed between BAG3 expression and other clinicopathological variables (Table I). Furthermore, a positive correlation between expressions of HSF1 and BAG3 was found in HCC ($P < 0.05$; Figure 5D) and patients with tumors showing BAG3 overexpression displayed significantly shorter overall survival (median: 84.0 months) compared with those patients whose tumors showed BAG3 low expression (median: 134.2 months; $P = 0.015$, log-rank test) (Figure 5E). Multivariate Cox regression

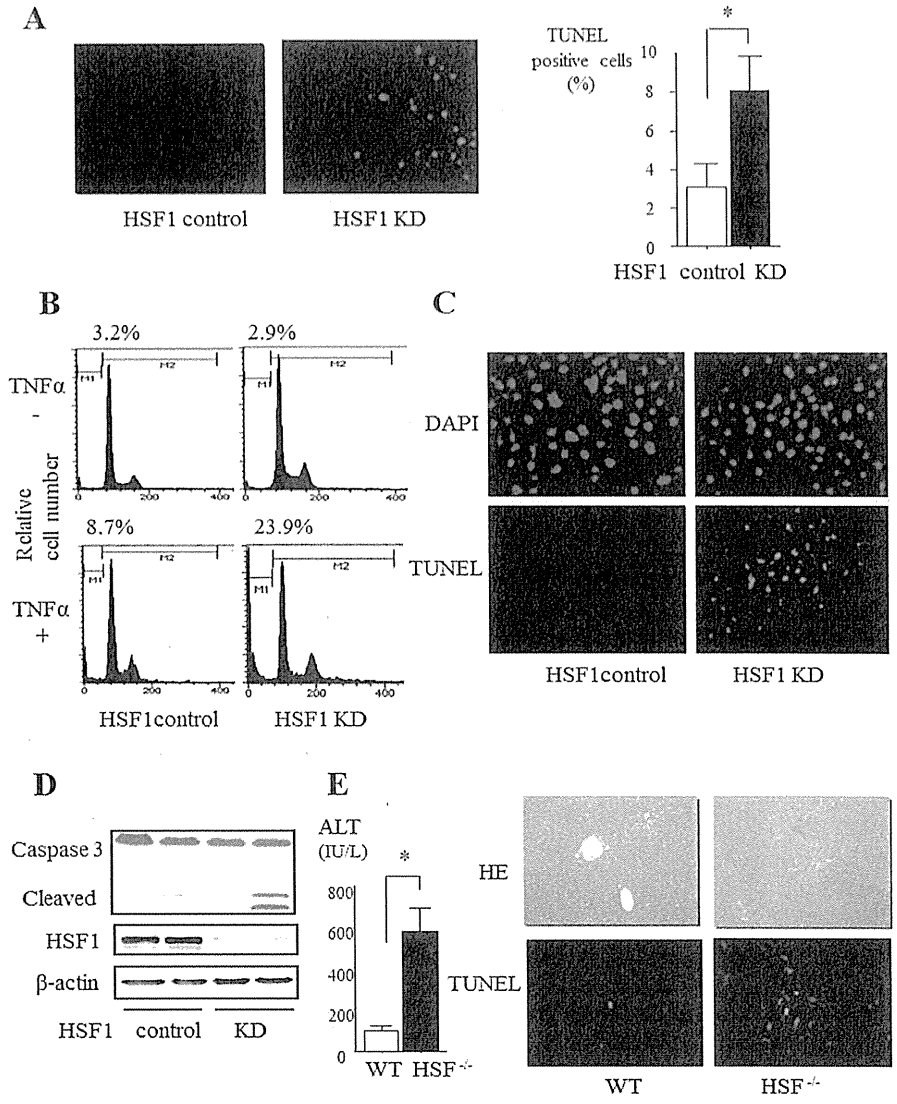

Fig. 3. Antiapoptotic effect of HSF1 in HCC cells and hepatocytes. (**A**) TUNEL staining was performed in tumors of HSF1 control and HSF1 KD cells from orthotopic implanted mice (left panel). TUNEL-positive cells were counted in tumors of HSF1 control and HSF1 KD cells. $*P < 0.05$. Bars: SEM (right panel). (**B**) Apoptotic cells were evaluated by FACS at 24 h after incubation with TNF-α (30 ng/ml). Values indicate percentages of cells with sub-G_1 DNA content. Representative data are shown from three independent experiments. (**C**) TUNEL staining was performed in HSF1 control and KD cells after incubation with TNF-α. (**D**) Protein expressions of caspase 3, HSF1 and β-actin in TNF-α-treated HSF1 control and KD cells were determined by western blot analysis. (**E**) Serum ALT levels 7 h after injection of WT and $HSF1^{-/-}$ mice with LPS (5 μg/kg) and GalN (500 mg/kg). $*P < 0.05$, compared with WT mice (left panel). HE and TUNEL stainings were performed in sections of livers obtained 7 h after injecting LPS (5 μg/kg) and GalN (500 mg/kg) into WT and $HSF1^{-/-}$ mice (right panel). ALT, alanine aminotransferase; DAPI, 4′,6-diamidino-2-phenylindole; HE, hematoxylin and eosin.

analysis identified high HSF1 expression (hazard ratio: 2.07; $P = 0.04$) as an independent prognostic factor for overall survival (Table II).

Discussion

As a master regulator of the heat shock response, HSF1 enhances organism survival and longevity in the face of environmental challenges. However, HSF1 can also act to the detriment of organisms by supporting malignant transformation (34). As reported previously, loss of HSF1 negatively impacts tumorigenesis driven by p53 or Ras mutations (8,16). Since HSF1 does not act as a classic oncogene, the increased resistance to proteotoxic stress induced by HSF1 was suggested to support tumor initiation and growth by enabling cells to accommodate the genetic alterations that accumulate during malignancy (35). However, the specific mechanisms by which HSF1 may support the growth of tumors are not well understood. Here, we have demonstrated that HSF1 has detrimental effects on liver tumor growth. We also proposed that the antiapoptotic effect of HSF1 may play a role in HCC tumor growth.

To clarify the mechanisms underlying this effect, we investigated associations between HSF1 and the NF-κB signaling pathway. Although, in a previous study, heat shock blocked the degradation of IκB (36) and nuclear translocation of NF-κB, the recent literature has reported that the presence of constitutively active HSF1 does not block TNF-α-induced activation of the NF-κB pathway or expression of a set of NF-κB-dependent genes (37). The current study established HSF1 KD cells and showed that HSF1 was necessary for TNF-α-induced NF-κB activation. We analyzed the function of BAG3 as a candidate for the molecule connecting HSF1 with NF-κB activation. BAG3 has reportedly been characterized by the

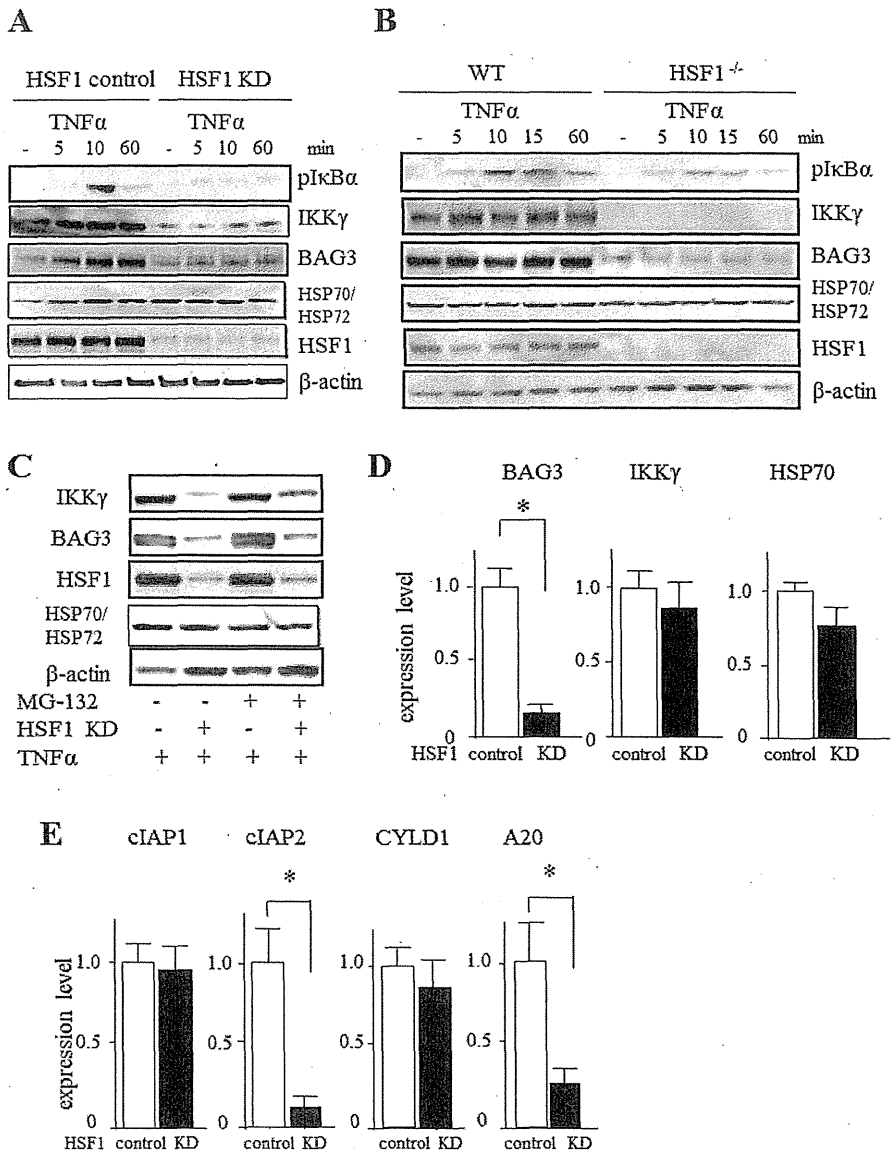

Fig. 4. HSF1 is involved in TNF-α-mediated NF-κB activation. (**A**) HSF1 control and KD cells were treated with TNF-α (30 ng/ml), lysed at the indicated times, gel separated and immunoblotted with antibodies against the indicated proteins. (**B**) HSF1 WT and HSF$^{-/-}$ hepatocytes treated with TNF-α (30 ng/ml), lysed at the indicated times, gel separated and immunoblotted with antibodies against the indicated proteins. (**C**) HSF1 control and KD cells were treated with TNF-α (30 ng/ml) with or without MG-132, lysed at 24 h, gel separated and immunoblotted with antibodies against indicated proteins. (**D**) Relative mRNA levels for BAG3, IKKγ and HSP70 in HSF1 control and KD cells determined by real-time PCR. Data are expressed as mean ± SEM ($n = 4$ per group). *$P < 0.05$. Bars: SEM. (**E**) Relative mRNA levels for antiapoptosis-related gene in HSF1 control and KD cells as determined by real-time PCR. Data are expressed as mean ± SEM ($n = 4$ per group). *$P < 0.05$. Bars: SEM. CYLD, cylindromatosis.

interaction with a variety of partners (Raf-1, steroid hormone receptors and HSP70) and is involved in regulating a number of cellular processes, particularly those associated with antiapoptosis (38). This molecule was expressed in response to stressful stimuli in a number of normal cell types and appears constitutively in a variety of tumors (33,39), and gene expression is regulated by HSF1 (40). In addition, knockdown of BAG3 protein decreased IKKγ levels, increasing tumor cell apoptosis and inhibiting tumor growth (33). Based on these considerations, we investigated whether attenuating HSF1 would enhance IKKγ protein expression, and data with MG-132 show that proteasomal degradation of IKKγ is enhanced in HSF1 KD cells. In addition, knowledge of the role BAG3 plays in preventing the proteasomal turnover of certain proteins suggests that the loss of BAG3 in HSF1 KD cells may be responsible for the enhanced turnover of IKKγ in this setting.

NF-κB activation is a master regulatory step in antiapoptosis. Several mechanisms have been reported regarding this antiapoptotic effect of NF-κB activation (41). NF-κB exerts its prosurvival activity primarily through the induction of target genes, the products of which inhibit components of the apoptotic machinery. These include Bcl-X_L and c-IAP (41), which binds directly to and inhibits the effect of caspases. This study showed that inactivation of NF-κB promoted apoptotic effects against TNF-α in HSF1$^{-/-}$ hepatocytes and HSF1 KD HCC cells. Real-time PCR analyses indicated that expression levels of apoptosis-related genes such as A20 and c-IAP2 were decreased by inhibition of NF-κB activation, whereas apoptosis-related genes such

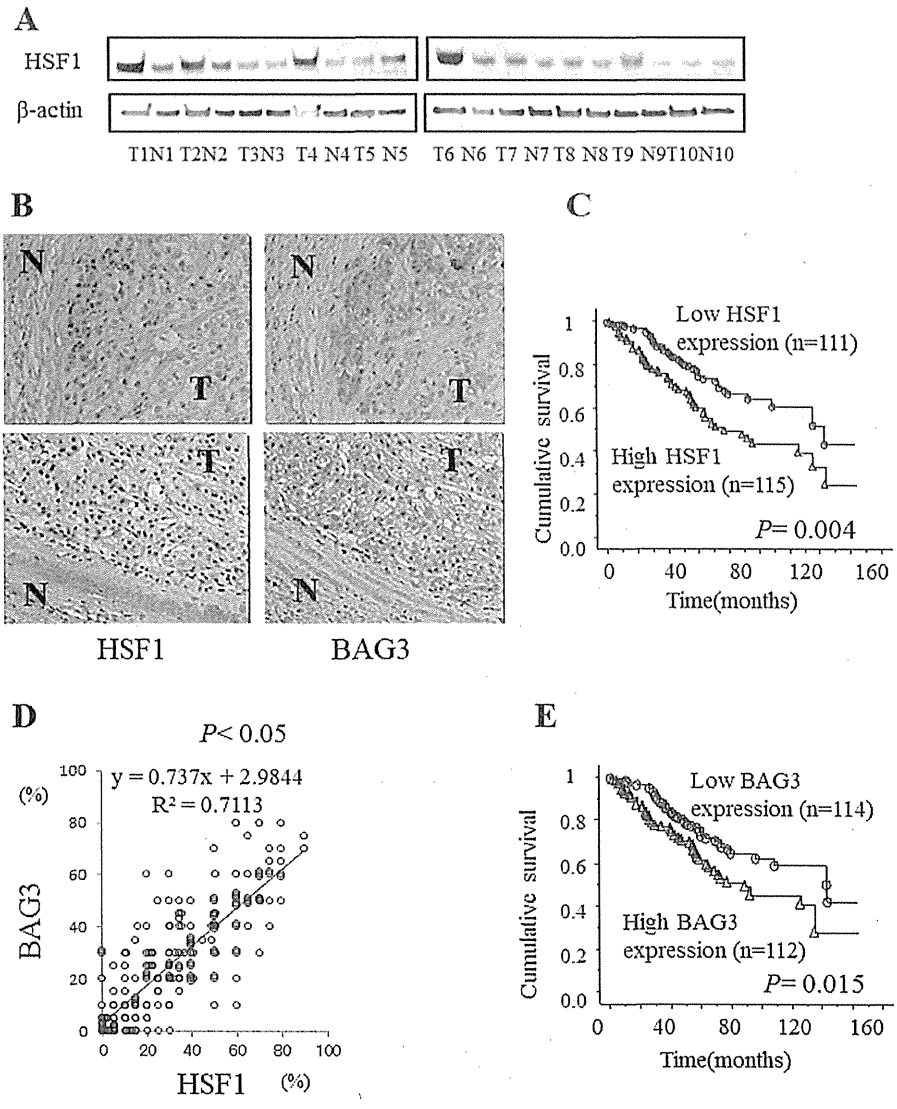

Fig. 5. Overexpression of HSF1 protein in human HCCs and pathological relationship between HSF1 and BAG3 in HCC samples. (**A**) HSF1 protein expression was determined in paired samples of human non-neoplastic liver and HCC by western blot, using β-actin as a control. N, non-cancerous liver; T, tumor. (**B**) Representative HSF1 and BAG3 staining of HCC and surrounding tissue. (**C**) Correlation of HSF1 overexpression with overall survival rates of patients. (**D**) Relationship between BAG3 and HSF1 expression in HCC. Scatterplot of BAG3 versus HSF1 with regression line displaying a correlation according to Spearman's correlation coefficient ($P < 0.01$). (**E**) Correlation of BAG3 overexpression with overall survival rates of patients.

as cIAP1 and cylindromatosis, which are known to be regulated by NF-κB activation, were apparently unaffected. Whether gene expression regulated by NF-κB activity differs between inducible and basal activation remains to be determined.

Regarding the relationship between HSF1 and HCC development, HSF1-deficient mice recently revealed dramatically reduced numbers and sizes of tumors compared with WT controls when tumors were induced by the chemical carcinogen, diethylnitrosamine. The same study suggested that the presence of extensive pathology associated with severe steatosis by diethylnitrosamine was prevented by HSF1 deletion and may be associated with reduced HCC development (42). On the other hand, ablation of IKKγ in liver parenchymal cells caused spontaneous development of HCC in mice, with tumor development preceded by steatohepatitis (43). Based on these observations, we assume that reductions in diethylnitrosamine-induced HCC development among HSF1-deficient mice may be associated with reduced expression of IKKγ, the reduction of which caused the steatosis.

BAG3 is a critical regulator of apoptosis in HSF1-deficient hepatocytes and HSF1 KD HCC cells. Moreover, the relationship between HSF1 and BAG3 has been shown not only in cell cultures and mouse models, but also in human HCC tissue samples; a correlation between HSF1 expression and BAG3 expression was found in HCC. Clinicopathological features and biological results provide a mechanistic link between HSF1 and HCC development via BAG3.

As for the ERK signal, a previous study demonstrated that impairment of JNK and ERK signaling in HSF1$^{-/-}$ MEF cells was caused in part by the reduced expression of EGFR (33). We showed a slight decrease in expression of EGFR among HSF1-deficient hepatocytes and HSF1 KD cells. On the other hand, the level of reduced activation of ERK, as a downstream molecule of EGFR, was larger than expected. However, the detailed mechanisms by which HSF1 regulates MAPK need further investigation.

In conclusion, we found that HSF1 deficiency significantly diminished NF-κB and MAPK activation in HCC hepatocytes and

Table II. Multivariate analysis with a Cox proportional hazards regression model

Characteristic	Univariate analysis	Multivariate analysis	Hazard ratio (95% CI)
Age (≥60 years)	0.22	0.15	
Gender (male)	0.92	0.53	
HCV status (positive)	0.28	0.82	
Cirrhosis (positive)	0.15	0.066	
Tumor size (≥50 mm)	<0.01*	0.011*	2.21 (1.18–4.12)
No. of tumor nodule (multiple)	<0.01*	<0.01*	2.67 (1.38–5.62)
Tumor differentiation (poor)	<0.01*	0.031*	2.34 (1.33–4.11)
Capsular formation (absence)	0.18	0.36	
Vascular invasion (presence)	0.062	0.10	
TNM stage (III + IV versus I + II)	<0.01*	0.020*	2.35 (1.14–4.82)
AFP (≥20 ng/ml)	0.18	0.36	
HSF1 expression (high)	0.018*	0.040*	2.07 (1.22–3.50)
BAG3 expression (high)	0.043*	0.056	

AFP, alpha-fetoprotein; CI, confidence interval; HCV, hepatitis C virus; TNM, tumor node metastasis.
*Significant *P* value.

HCC cells; accordingly, HSF1 deficiency inhibited the development of HCC. Furthermore, clinicopathological analysis demonstrated a significant correlation between HSF1 or BAG3 protein levels and prognosis. Our results demonstrate the importance of HSF1 in human HCCs and suggest inhibition of HSF1 as a novel strategy to target that subset of HCC patients in whom this protein is overexpressed.

Supplementary material

Supplementary Materials and methods, Table I and Figures 1 and 2 can be found at http://carcin.oxfordjournals.org/

Funding

Ministry of Education, Culture, Sports, Science and Technology, Japan (to N.S.); Japan Society for the Promotion of Science (24390185, 24659359); Ministry of Health, Labour and Welfare Japan; Japan Health Sciences Foundation; grants-in-aid for scientific research (22300317) and Uehara Memorial Foundation (to S.M.).

Conflict of Interest Statement: None declared.

References

1. El-Serag,H.B. (2012) Epidemiology of viral hepatitis and hepatocellular carcinoma. *Gastroenterology*, **142**, 1264–1273.e1.
2. Cheng,A.L. *et al.* (2009) Efficacy and safety of sorafenib in patients in the Asia-Pacific region with advanced hepatocellular carcinoma: a phase III randomised, double-blind, placebo-controlled trial. *Lancet Oncol.*, **10**, 25–34.
3. Breuhahn,K. *et al.* (2011) Strategies for hepatocellular carcinoma therapy and diagnostics: lessons learned from high throughput and profiling approaches. *Hepatology*, **53**, 2112–2121.
4. Pirkkala,L. *et al.* (2001) Roles of the heat shock transcription factors in regulation of the heat shock response and beyond. *FASEB J.*, **15**, 1118–1131.
5. Sorger,P.K. (1991) Heat shock factor and the heat shock response. *Cell*, **65**, 363–366.
6. Guertin,M.J. *et al.* (2010) Chromatin landscape dictates HSF binding to target DNA elements. *PLoS Genet.*, **6**, e1001114.
7. Mendillo,M.L. *et al.* (2012) HSF1 drives a transcriptional program distinct from heat shock to support highly malignant human cancers. *Cell*, **150**, 549–562.
8. Page,T.J. *et al.* (2006) Genome-wide analysis of human HSF1 signaling reveals a transcriptional program linked to cellular adaptation and survival. *Mol. Biosyst.*, **2**, 627–639.
9. Dai,C. *et al.* (2007) Heat shock factor 1 is a powerful multifaceted modifier of carcinogenesis. *Cell*, **130**, 1005–1018.
10. Hayashida,N. *et al.* (2006) A novel HSF1-mediated death pathway that is suppressed by heat shock proteins. *EMBO J.*, **25**, 4773–4783.
11. Jacobs,A.T. *et al.* (2007) Heat shock factor 1 attenuates 4-hydroxynonenal-mediated apoptosis: critical role for heat shock protein 70 induction and stabilization of Bcl-XL. *J. Biol. Chem.*, **282**, 33412–33420.
12. Vydra,N. *et al.* (2006) Spermatocyte-specific expression of constitutively active heat shock factor 1 induces HSP70i-resistant apoptosis in male germ cells. *Cell Death Differ.*, **13**, 212–222.
13. Neckers,L. *et al.* (2012) Hsp90 molecular chaperone inhibitors: are we there yet? *Clin. Cancer Res.*, **18**, 64–76.
14. Khalil,A.A. *et al.* (2011) Heat shock proteins in oncology: diagnostic biomarkers or therapeutic targets? *Biochim. Biophys. Acta*, **1816**, 89–104.
15. Chuma,M. *et al.* (2003) Expression profiling in multistage hepatocarcinogenesis: identification of HSP70 as a molecular marker of early hepatocellular carcinoma. *Hepatology*, **37**, 198–207.
16. Cai,L. *et al.* (2003) The tumor-selective over-expression of the human Hsp70 gene is attributed to the aberrant controls at both initiation and elongation levels of transcription. *Cell Res.*, **13**, 93–109.
17. Min,J.N. *et al.* (2007) Selective suppression of lymphomas by functional loss of Hsf1 in a p53-deficient mouse model for spontaneous tumors. *Oncogene*, **26**, 5086–5097.
18. Santagata,S. *et al.* (2011) High levels of nuclear heat-shock factor 1 (HSF1) are associated with poor prognosis in breast cancer. *Proc. Natl Acad. Sci. USA*, **108**, 18378–18383.
19. Dudeja,V. *et al.* (2011) Prosurvival role of heat shock factor 1 in the pathogenesis of pancreatobiliary tumors. *Am. J. Physiol. Gastrointest. Liver Physiol.*, **300**, G948–G955.
20. Hoang,A.T. *et al.* (2000) A novel association between the human heat shock transcription factor 1 (HSF1) and prostate adenocarcinoma. *Am. J. Pathol.*, **156**, 857–864.
21. Ishiwata,J. *et al.* (2012) State of heat shock factor 1 expression as a putative diagnostic marker for oral squamous cell carcinoma. *Int. J. Oncol.*, **40**, 47–52.
22. Kojiro,M. *et al.* (2009) Pathologic diagnosis of early hepatocellular carcinoma: a report of the international consensus group for hepatocellular neoplasia. *Hepatology*, **49**, 658–664.
23. Fabregat,I. *et al.* (2007) Survival and apoptosis: a dysregulated balance in liver cancer. *Liver Int.*, **27**, 155–162.
24. Nakagawa,H. *et al.* (2011) Apoptosis signal-regulating kinase 1 inhibits hepatocarcinogenesis by controlling the tumor-suppressing function of stress-activated mitogen-activated protein kinase. *Hepatology*, **54**, 185–195.
25. Sun,B. *et al.* (2008) NF-kappaB signaling, liver disease and hepatoprotective agents. *Oncogene*, **27**, 6228–6244.
26. Maeda,S. *et al.* (2005) IKKbeta couples hepatocyte death to cytokine-driven compensatory proliferation that promotes chemical hepatocarcinogenesis. *Cell*, **121**, 977–990.
27. Beeram,M. *et al.* (2005) Raf: a strategic target for therapeutic development against cancer. *J. Clin. Oncol.*, **23**, 6771–6790.
28. Whittaker,S. *et al.* (2010) The role of signaling pathways in the development and treatment of hepatocellular carcinoma. *Oncogene*, **29**, 4989–5005.
29. Inouye,S. *et al.* (2003) Activation of heat shock genes is not necessary for protection by heat shock transcription factor 1 against cell death due to a single exposure to high temperatures. *Mol. Cell. Biol.*, **23**, 5882–5895.
30. Chuma,M. *et al.* (2004) Overexpression of cortactin is involved in motility and metastasis of hepatocellular carcinoma. *J. Hepatol.*, **41**, 629–636.
31. O'Callaghan-Sunol,C. *et al.* (2006) Heat shock transcription factor (HSF1) plays a critical role in cell migration via maintaining MAP kinase signaling. *Cell Cycle*, **5**, 1431–1437.

32. Nowak,M. *et al.* (2000) LPS-induced liver injury in D-galactosamine-sensitized mice requires secreted TNF-alpha and the TNF-p55 receptor. *Am. J. Physiol. Regul. Integr. Comp. Physiol.*, **278**, R1202–R1209.
33. Ammirante,M. *et al.* (2010) IKK{gamma} protein is a target of BAG3 regulatory activity in human tumor growth. *Proc. Natl Acad. Sci. USA*, **107**, 7497–7502.
34. Meng,L. *et al.* (2010) Heat-shock transcription factor HSF1 has a critical role in human epidermal growth factor receptor-2-induced cellular transformation and tumorigenesis. *Oncogene*, **29**, 5204–5213.
35. Solimini,N.L. *et al.* (2007) Non-oncogene addiction and the stress phenotype of cancer cells. *Cell*, **130**, 986–988.
36. Malhotra,V. *et al.* (2002) Heat shock inhibits activation of NF-kappaB in the absence of heat shock factor-1. *Biochem. Biophys. Res. Commun.*, **291**, 453–457.
37. Janus,P. *et al.* (2011) NF-κB signaling pathway is inhibited by heat shock independently of active transcription factor HSF1 and increased levels of inducible heat shock proteins. *Genes Cells*, **16**, 1168–1175.
38. Rosati,A. *et al.* (2011) BAG3: a multifaceted protein that regulates major cell pathways. *Cell Death Dis.*, **2**, e141.
39. Homma,S. *et al.* (2006) BAG3 deficiency results in fulminant myopathy and early lethality. *Am. J. Pathol.*, **169**, 761–773.
40. Franceschelli,S. *et al.* (2008) Bag3 gene expression is regulated by heat shock factor 1. *J. Cell. Physiol.*, **215**, 575–577.
41. Luo,J.L. *et al.* (2005) IKK/NF-kappaB signaling: balancing life and death–a new approach to cancer therapy. *J. Clin. Invest.*, **115**, 2625–2632.
42. Jin,X. *et al.* (2011) Heat shock transcription factor 1 is a key determinant of HCC development by regulating hepatic steatosis and metabolic syndrome. *Cell Metab.*, **14**, 91–103.
43. Luedde,T. *et al.* (2007) Deletion of NEMO/IKKgamma in liver parenchymal cells causes steatohepatitis and hepatocellular carcinoma. *Cancer Cell*, **11**, 119–132.

Received December 4, 2012; revised August 22, 2013; accepted August 28, 2013

J Gastroenterol
DOI 10.1007/s00535-014-1023-2

The Japanese Society of Gastroenterology

ORIGINAL ARTICLE—LIVER, PANCREAS, AND BILIARY TRACT

Association of serum IFN-λ_3 with inflammatory and fibrosis markers in patients with chronic hepatitis C virus infection

Yoshihiko Aoki · Masaya Sugiyama · Kazumoto Murata · Sachiyo Yoshio · Masayuki Kurosaki · Satoru Hashimoto · Hiroshi Yatsuhashi · Hideyuki Nomura · Jong-Hon Kang · Tsutomu Takeda · Shigeko Naito · Tatsuji Kimura · Yoko Yamagiwa · Masaaki Korenaga · Masatoshi Imamura · Naohiko Masaki · Namiki Izumi · Masayoshi Kage · Masashi Mizokami · Tatsuya Kanto

Received: 22 September 2014 / Accepted: 20 November 2014

Abstract
Background Hepatitis C virus (HCV) is one of the major causes of liver cancer. The single nucleotide polymorphisms within the *IFNL3* gene, which encodes interferon (IFN)-λ_3, are strongly associated with the response to pegylated IFN-α (PEG-IFN-α) plus ribavirin (RBV) therapy in chronic hepatitis C (C-CH) patients. However, the roles of IFN-λ_3 in chronic HCV infection are still elusive. In this study, we aimed to identify clinical and immunological factors influencing IFN-λ_3 and evaluated whether serum IFN-λ_3 levels are involved or not involved in the response to PEG-IFN-α plus RBV therapy.

Methods We enrolled 119 C-CH patients with HCV genotype 1 infection who underwent 48 weeks of PEG-IFN-α plus RBV therapy. As controls, 23 healthy subjects and 56 patients with non-HCV viral hepatitis were examined. Serum IFN-λ_3 was quantified by chemiluminescence enzyme immunoassay, and 27 cytokines or chemokines were assayed by the multiplexed BioPlex system.
Results Serum IFN-λ_3 levels were higher in C-CH patients or acute hepatitis E patients than in healthy volunteers. Such levels did not differ between the *IFNL3* genotypes. In C-CH patients, serum IFN-λ_3 was positively correlated with aspartate aminotransferase, alanine aminotransferase, α-fetoprotein, histological activity, fibrosis index, IFN-γ-inducible protein 10, and platelet-derived growth factor. Multivariate analysis showed that *IFNL3* single nucleotide polymorphisms, fibrosis score, and macrophage inflammatory protein 1α were involved in the

Y. Aoki and M. Sugiyama contributed equally to this work.

Electronic supplementary material The online version of this article (doi:10.1007/s00535-014-1023-2) contains supplementary material, which is available to authorized users.

Y. Aoki · M. Sugiyama · K. Murata · S. Yoshio · Y. Yamagiwa · M. Korenaga · M. Imamura · N. Masaki · M. Mizokami · T. Kanto (✉)
Department of Hepatic Diseases, The Research Center for Hepatitis and Immunology, National Center for Global Health and Medicine, 1-7-1 Kohnodai, Ichikawa, Chiba 272-8516, Japan
e-mail: kantot@hospk.ncgm.go.jp

M. Kurosaki · N. Izumi
Department of Gastroenterology and Hepatology, Musashino Red Cross Hospital, Tokyo, Japan

S. Hashimoto · H. Yatsuhashi
National Hospital Organization Nagasaki Medical Center, Clinical Research Center, Omura, Japan

H. Nomura
The Center for Liver Diseases, Shin-Kokura Hospital, Kitakyushu, Japan

J.-H. Kang
Center for Gastroenterology, Teine Keijinkai Hospital, Sapporo, Japan

T. Takeda
Department of Gastroenterology, Juntendo University School of Medicine, Tokyo, Japan

S. Naito · T. Kimura
Institute of Immunology Co. Ltd, Tokyo, Japan

M. Kage
Department of Diagnostic Pathology, Kurume University Medical School, Fukuoka, Japan

Published online: 14 December 2014

sustained viral clearance in PEG-IFN-α plus RBV therapy; however, serum IFN-λ_3 levels were not involved.
Conclusion Serum IFN-λ_3 levels are increased in C-CH patients regardless of the *IFNL3* genotype. IFN-λ_3 is a biomarker reflecting the activity and fibrosis of liver disease, but is not correlated with the responsiveness to PEG-IFN-α plus RBV therapy.

Keywords Hepatitis C virus · IL-28B · Interferon-λ_3 · Chemokine · Pegylated interferon-α plus ribavirin

Abbreviations

APRI	Aspartate aminotransferase platelet ratio index
ALT	Alanine aminotransferase
AST	Aspartate aminotransferase
B-CH	Chronic hepatitis B
C-CH	Chronic hepatitis C
FIB-4	Fibrosis-4
HBV	Hepatitis B virus
HCC	Hepatocellular carcinoma
HCV	Hepatitis C virus
HIV	Human immunodeficiency virus
HV	Healthy volunteer
IFN	Interferon
IP-10	Interferon-γ-inducible protein 10
MIP	Macrophage inflammatory protein
PDGF-BB	Platelet-derived growth factor BB
PEG-IFN-α	Pegylated interferon-α
RANTES	Regulated on activation, normally T cell expressed, and secreted
RBV	Ribavirin
SNP	Single nucleotide polymorphism
SVR	Sustained virological response

Introduction

Hepatitis C virus (HCV) is one of the leading causes of liver cirrhosis and hepatocellular carcinoma (HCC), with nearly 170 million people infected worldwide [1]. A combination therapy with pegylated interferon (IFN)-α (PEG-IFN-α) and ribavirin (RBV) has been used for chronic hepatitis C (C-CH) patients as the standard of care, achieving sustained virological response (SVR) in 42–52 % of genotype 1 patients [2]. Even in the coming era of all oral and IFN-free regimens for the treatment of C-CH patients [3–5], PEG-IFN-α plus RBV therapy could hold promise for elderly patients with advanced fibrosis and high risk of HCC.

Genome-wide association studies, including ours, have demonstrated that single nucleotide polymorphisms (SNPs) upstream of the promoter region within the *IFNL3* gene (also known as *IL28B*), which encodes a type III IFN (IFN-λ_3), are strongly associated with the response to PEG-IFN-α plus RBV therapy in C-CH patients [6–9]. Although such significant impact of the *IFNL3* genotype on the outcome of the combination therapy is well acknowledged, the biological and clinical roles of IFN-λ_3 in chronic HCV infection are still elusive. Furthermore, it is controversial if patients with the *IFNL3* major genotype are capable of producing larger amounts of IFN-λ_3 than those with the minor genotype.

The IFN-λ family consists of several subtypes, such as IFN-λ_1 (IL-29), IFN-λ_2 (IL-28A), and IFN-λ_3 (IL-28B), which are biologically active for the suppression of HCV replication [10, 11]. On initial exposure to HCV, primary human hepatocytes in vitro produced IFN-λ and subsequently induced antiviral IFN-stimulated genes [12]. It is thus rational to consider that the more IFN-λ family members are produced in the exposed hosts, the more likely they are to protect the hosts from HCV virulence in the primary infection. However, in chronically HCV-infected patients, it has not been proven that such a scenario could be applicable for the outcome of the disease.

To gain insight into the role of IFN-λ_3 in chronic HCV infection, we aimed to clarify the factors influencing serum IFN-λ_3 levels, including *IFNL3* genotype, clinical parameters, and various cytokines and chemokines. For application in clinical practice, we evaluated whether serum IFN-λ_3 levels are associated or not associated with the response to PEG-IFN-α plus RBV therapy for C-CH patients.

Materials and methods

Study subjects

One hundred nineteen Japanese patients with C-CH (genotype 1b and high viral load) were enrolled in the study. All patients were negative for hepatitis B virus (HBV) and human immunodeficiency virus (HIV) and did not have any other chronic liver diseases, such as alcoholic, autoimmune, and fatty liver disease. The presence of HCC was ruled out by ultrasonography or computed tomography examinations. The patients had been followed at the National Center for Global Health and Medicine Kohnodai Hospital, the National Hospital Organization Nagasaki Medical Center, Shin-Kokura Hospital, and Musashino Red Cross Hospital. They were treated with PEG-IFN-α_{2b} (subcutaneously once a week; 1.5 μg/kg body weight) or PEG-IFN-α_{2a} (180 μg once a week) plus RBV (600–1,000 mg daily depending on body weight) for 48 weeks according to the guidelines of the Japan Society of Hepatology [13]. Virological response to the combination therapy was defined according to the practical

guidelines of the American Association for the Study of Liver Diseases [14]. All patients attained adherence to PEG-IFN-α plus RBV therapy exceeding 80 % of the estimated total dose. Liver biopsy was performed before the start of the therapy. Histological activity and fibrosis were determined according to the METAVIR scoring system [15]. Serum samples were collected from the patients before PEG-IFN-α plus RBV treatment started and were stored at −80 °C. In some patients, the samples were obtained 24 weeks after the cessation of the therapy (at the end of follow-up).

As controls, serum was obtained from 23 healthy subjects without HCV, HBV, and HIV infection (male-to-female ratio, 5:5, mean age ± standard deviation, 45 ± 12 years). In the comparison of serum IFN-λ levels between C-CH patients and patients with other types of liver diseases, 11 patients with chronic HBV infection (three HBeAg-positive patients and eight HBeAg-negative patients) were examined as well. They were not treated with IFN or nucleot(s)ide analogues for HBV infection. In addition, we compared serum IFN-λ_3 levels among patients with acute viral hepatitis of various causes, such as acute hepatitis A, acute hepatitis B, or acute hepatitis E, the diagnosis of which was determined by serological examinations at Teine Keijinkai Hospital and Kurume University Hospital. The serum samples were obtained from the patients at the time of active liver inflammation [alanine aminotransferase (ALT) levels more than two times the upper limit of the normal range]. As representatives for noninvasive fibrosis markers, the fibrosis-4 (FIB-4) score and the aspartate aminotransferase (AST) platelet ratio index (APRI) were calculated as reported previously [16, 17].

The study protocol conformed to the ethical guidelines of the 1975 Declaration of Helsinki and was approved by the Institutional Review Board at the National Center for Global Health and Medicine (approval ID and date, NCGM-G-001379-00, March 14, 2013) and the ethical committee of each institute. Written informed consent was obtained from all patients.

IFNL3 genotyping

The subjects were evaluated for SNPs near the *IFNL3* gene (rs8099917) using the Invader Plus assay (Invader Chemistry, Madison, WI, USA) as previously reported [18]. The TT, TG, and GG genotypes were determined accordingly.

Measurement of serum IFN-λ_3

Serum levels of IFN-λ_3 were evaluated by the newly developed chemiluminescence enzyme immunoassay system as reported previously [19]. The system enables one to quantify serum IFN-λ_3 specifically without any overlap from IFN-λ_1 and IFN-λ_2. The threshold of the assay is 10 pg/mL and its range is 10–1,000 pg/mL.

Simultaneous measurement of multiple chemokines and cytokines

To quantify multiple chemokines and cytokines simultaneously in the limited volume of the samples, we used the BioPlex 3D system (BioPlex Pro Human GI 27Plex; Bio-Rad, Hercules, CA, USA) for the study. In this system, 27 chemokines and cytokines were measurable, such as basic fibroblast growth factor, eotaxin, granulocyte colony stimulating factor, granulocyte–macrophage colony stimulating factor, IL-1β, IL-1 receptor antagonist, IL-2, IL-4, IL-5, IL-6, IL-7, IL-8, IL-9, IL-10, IL-12, IL-13, IL-15, IL-17, IFN-γ, IFN-γ-inducible protein 10 (IP-10), monocyte chemotactic protein 1, macrophage inflammatory protein (MIP)-1α, MIP-1β, platelet-derived growth factor BB (PDGF-BB), regulated on activation, normally T cell expressed, and secreted (RANTES), TNF-α, and vascular endothelial growth factor. The detection range and thresholds are given in Table S1. For the measurement of IP-10, ELISA (R&D Systems, MN, USA) was performed as well.

Statistical analyses

Continuous variables were compared between groups using the Wilcoxon signed-rank test and the Mann–Whitney *U* test, and categorical data were compared using the χ^2 test or Fisher's exact test. The correlations between cytokines, chemokines, and clinical markers were evaluated by Spearman's correlation coefficient. A p value below 0.05 was considered to be significant. Logistic regression was used for multivariate analyses. All statistical analyses were performed with PRISM and SPSS.

Results

Serum IFN-λ_3 levels are increased in patients with chronic HCV infection

The clinical backgrounds of C-CH patients are shown in Table 1. First, we compared serum IFN-λ_3 levels among patients with C-CH or chronic hepatitis B (B-CH) and uninfected healthy volunteers (HVs). Such levels in the C-CH group were significantly higher than those in the B-CH group or the HV group (Fig. 1a). The levels in the B-CH group were increased, but the significance of this was much less than in the C-CH group (Fig. 1a). When we compared serum IFN-λ_3 levels in B-CH patients between

Table 1 Clinical backgrounds of the patients with chronic hepatitis C virus (*HCV*) infection

Factors	Values
Number	119 (69 male, 50 female)
Age (years)	56.5 ± 10.1
WBC (/mm^3)	5,120 ± 1,575
Hb (g/dL)	14.4 ± 1.5
Plt (×10^4/mm^3)	17.7 ± 5.2
TP (g/dL)	7.5 ± 0.5
Alb (g/dL)	4.2 ± 0.4
AST (U/L)	54.7 ± 38.3
ALT (U/L)	71.5 ± 54.2
T-bil (mg/dL)	0.8 ± 0.3
T-chol (mg/dL)	176.6 ± 37.0
AFP (ng/mL)	9.7 ± 13.4
HCV RNA (log IU/mL)	6.3 ± 0.6
Activity (A0/A1/A2/A3)	1/68/33/2
Fibrosis (F1/F2/F3/F4)	48/36/16/4
IFNL3 rs8099917 (TT/non-TT)	100:19

Alb albumin, *AFP* α-fetoprotein, *ALT* alanine aminotransferase, *AST* aspartate aminotransferase, *Hb* hemoglobin, *Plt* platelets, *T-bil* total bilirubin, *T-chol* total cholesterol, *TP* total protein, *WBC* white blood cells

HBeAg-positive and HBeAg-negative patients, we found no difference between them (2.5 ± 0.9 pg/mL vs 1.8 ± 1.7 pg/mL, respectively). Next, we compared serum IFN-λ_3 levels between patients with the *IFNL3* TT genotype and those with the TG/GG (non-TT) genotype in the C-CH group. Although some patients in the TT group showed relatively higher levels of IFN-λ_3 than those in the non-TT group, this difference between the TT and non-TT groups did not reach significance (Fig. 1b). Third, we compared serum IFN-λ_3 levels before and after the combination therapy in the relevant cases. In patients who successfully eradicated HCV (SVR), serum IFN-λ_3 levels were significantly decreased at 24 weeks after the therapy. In contrast, such levels did not change in those patients who failed to eradicate HCV (transient virological response and no virological response groups, respectively) (Fig. 1c). Fourth, we compared serum IFN-λ_3 levels among patients with various causes of acute viral hepatitis. Unfortunately, serum samples from acute hepatitis C patients were not available in this study. The IFN-λ_3 levels in the acute hepatitis E group were higher than those in the HVs (Fig. 1d). The IFN-λ_3 levels in the acute hepatitis B group tended to be higher than those in the HVs; however, statistical analysis was not performed because of the limited number of samples ($N = 2$). No significant difference was observed between the acute hepatitis A and HV groups. These results indicate that serum IFN-λ_3 levels are increased in patients with C-CH or acute hepatitis E.

Serum IFN-λ_3 levels may be related to liver inflammation or fibrosis in patients with C-CH

To explore the clinical significance of IFN-λ_3 in chronic HCV infection, we simultaneously examined 27 chemokines and cytokines in serum by means of the BioPlex system, which allows one to measure multiple factors at high sensitivity in a small volume of samples (10 μL per sample). In comparison with the results for HVs, we found that the levels of some chemokines in the C-CH group were higher than those in the HV group, such as IP-10, MIP-1α, MIP-1β, RANTES, and PDGF-BB (Figs. 2, S1).

Next, we examined whether serum IFN-λ_3 levels are correlated or not correlated with clinical parameters or immunological markers in the C-CH group. The IFN-λ_3 levels were weakly and positively correlated with AST, ALT, and α-fetoprotein levels and histological activity (Table 2). These results indicate that the increase of serum IFN-λ_3 levels in patients with C-CH is related to liver inflammation. The FIB-4 score and the APRI are representatives of noninvasive markers of liver fibrosis. The levels of serum IFN-λ_3 were positively correlated with the APRI, but not with the FIB-4 score (Table 2). With regard to the chemokines displaying higher values in the C–CH group, the levels of IP-10 and PDGF-BB were positively correlated with the IFN-λ_3 levels (Table 2). Such chemokines are reported to be involved in the early stage of liver fibrosis [20–22]. Thus, serum levels of IFN-λ_3 may be related to the fibrotic markers as well. To clarify the mechanisms causing the increase of serum IFN-λ_3 levels in B-CH patients, we examined the correlations between serum IFN-λ_3 levels and clinical markers and fibrosis indices. Serum IFN-λ_3 levels were correlated with the levels of AST ($r = 0.64$, $p = 0.03$) and total cholesterol ($r = -0.76$, $p = 0.03$), FIB-4 score ($r = 0.65$, $p = 0.03$), and APRI ($r = 0.76$, $p = 0.007$) (Table S2). In addition, serum IFN-λ_3 levels tended to be higher in HBV-positive patients with liver cirrhosis or HCC (3.0 ± 3.1 pg/mL in liver cirrhosis patients and 4.1 ± 4.7 pg/mL in HCC patients, respectively) (Fig. S2). These results show that serum IFN-λ_3 levels are related to liver inflammation and fibrosis not only in C-CH patients but also in B-CH patients.

Pretreatment serum IFN-λ_3 is not related to SVR to PEG-IFN-α plus RBV therapy in patients with C-CH

Because the *IFNL3* genotype is a strong predictor of the efficacy of PEG-IFN-α plus RBV therapy for C-CH, we sought to examine the clinical value of serum IFN-λ_3 in patients who underwent the combination therapy. In a comparison of the clinical and immunological factors between the SVR and non-SVR groups, univariate analysis

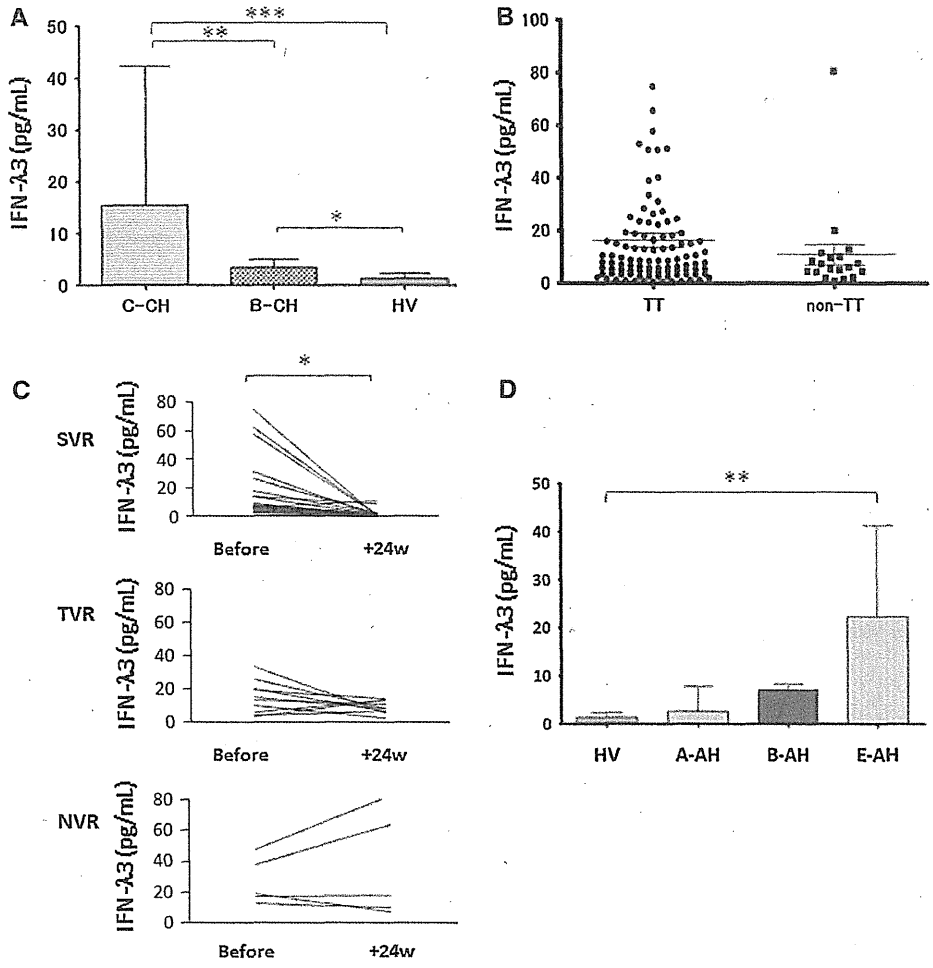

Fig. 1 Serum interferon-λ_3 (*IFN-λ3*) levels are increased in patients with chronic hepatitis C virus infection or acute hepatitis E virus infection. **a** Serum IFN-λ_3 levels in patients with chronic hepatitis C (*C–CH*; $N = 119$), patients with chronic hepatitis B (*B-CH*; $N = 11$), and healthy volunteers (*HV*; $N = 23$) were quantified by the chemiluminescence enzyme immunoassay (CLEIA) method as described in "Materials and methods." *One asterisk* $p < 0.05$, *two asterisks* $p < 0.01$, *three asterisks* $p < 0.0001$ by the Mann–Whitney *U* test. **b** Serum IFN-λ_3 levels in the C-CH group were compared between the patients with the *IFNL3* TT (rs8099917) genotype ($N = 100$) and those with non-TT (TG/GG) genotype ($N = 19$). **c** Serum IFN-λ_3 levels in C-CH patients were compared before and 24 weeks after the pegylated interferon-α plus ribavirin therapy. *SVR* sustained virological response ($N = 21$), *TVR* transient virological response ($N = 10$), *NVR* nonvirological response ($N = 5$), *one asterisk* $p < 0.05$ by Wilcoxon's signed-rank test. **d** Serum IFN-λ_3 levels in acute hepatitis patients of various causes were quantified by CLEIA as described in "Materials and methods." All samples were collected from patients whose alanine aminotransferase levels were two times higher than the upper limit of the normal range. *HV* healthy volunteers ($N = 23$), *A-AH* acute hepatitis A patients ($N = 34$), *B-AH* acute hepatitis B patients ($N = 2$), *E-AH* acute hepatitis E patients ($N = 9$), *two asterisks* $p < 0.0001$ by the Mann–Whitney *U* test

revealed that AST, *IFNL3* genotype, fibrosis score, and MIP-1α were associated with the SVR (Table 3). However, serum IFN-λ_3 or IP-10 levels were not different between the SVR and non-SVR groups (Table 3). Subsequently, multivariate analysis including such factors of significance ($p < 0.05$ by univariate analysis) showed that *IFNL3* SNPs, fibrosis score, and MIP-1α were involved in the SVR (Table 3). These results suggest that serum IFN-λ_3 fails to be a predictive marker for SVR in PEG-IFN-α plus RBV therapy.

Discussion

In this study, we demonstrated that serum IFN-λ_3 levels were higher in patients with C-CH than in uninfected or HBV-positive patients, the levels in whom did not differ regardless of the *IFNL3* genotype. Serum IFN-λ_3 levels were correlated with clinical and immunological markers of liver inflammation and fibrosis, suggesting that the production of IFN-λ_3 may be regulated by not only the presence or absence of HCV but also by the status of liver

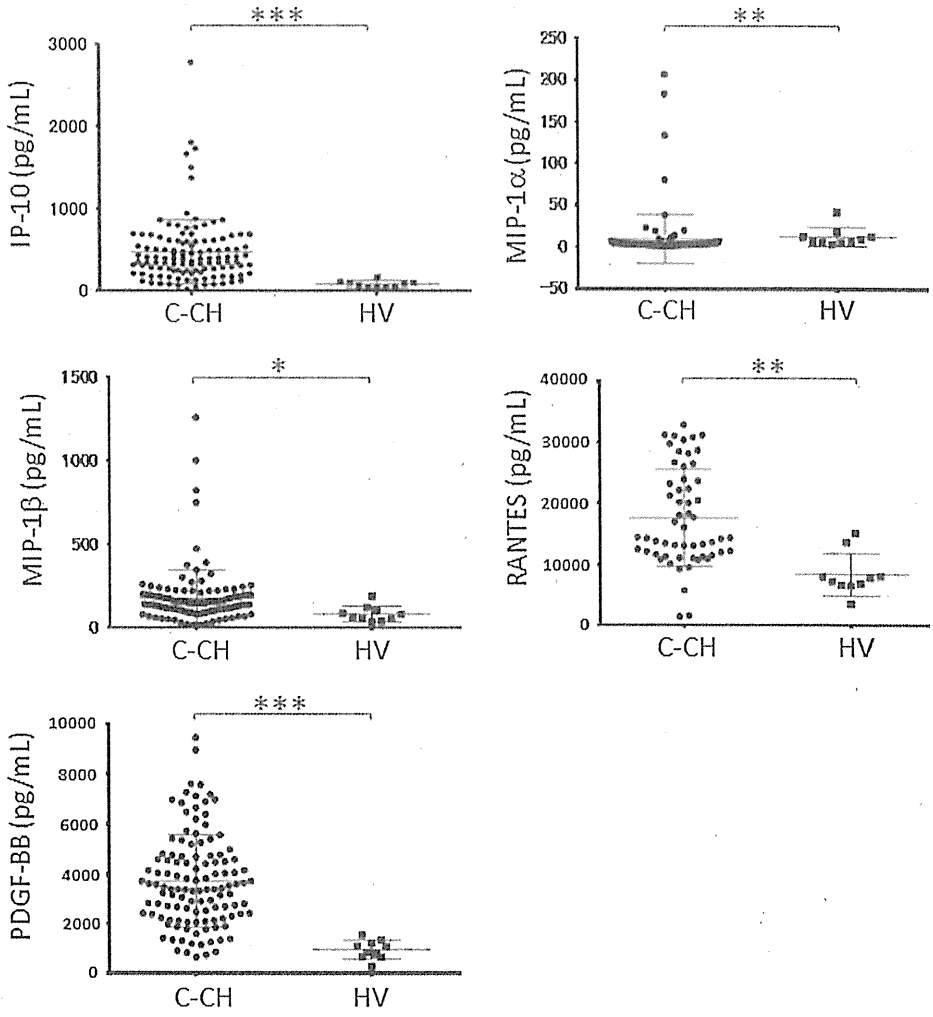

Fig. 2 The levels of several chemokines are increased in patients with chronic hepatitis C virus infection. Twenty-seven chemokines and cytokines in serum from chronic hepatitis C patients (*C-CH*) and healthy volunteers (*HV*) were assayed by means of the BioPlex method. Interferon-γ-inducible protein 10 (*IP-10*) was measured by ELISA. Representative results for chemokines that showed statistical significance between the groups are shown, such as IP-10, macrophage inflammatory protein 1α (*MIP-1α*), macrophage inflammatory protein 1β (*MIP-1β*), regulated on activation, normally T cell expressed, and secreted (*RANTES*), and platelet-derived growth factor BB (*PDGF-BB*). * $p < 0.005$, ** $p < 0.001$, *** $p < 0.0001$ by the Mann–Whitney *U* test

disease. It is well acknowledged that *IFNL3* genotype is a strong predictor of SVR in PEG-IFN-α plus RBV therapy for C-CH [7–9]. However, serum IFN-λ_3 fails to be a surrogate marker for *IFNL3* genotype in the combination therapy.

On primary HCV infection, IFN-λ is produced by hepatocytes that subsequently induce antiviral IFN-stimulated genes [23]. Parallel reduction of serum IFN-λ_3 levels in C-CH patients who attained SVR by PEG-IFN-α plus RBV treatment indicates that the presence of HCV is involved in the production of IFN-λ_3. In addition to hepatocytes, dendritic cells or macrophages are capable of producing IFN-λ in response to HCV [24]. For sensing HCV, hepatocytes and BDCA3$^+$ dendritic cells mainly utilize Toll-like receptor 3 and retinoic acid inducible gene I, and plasmacytoid dendritic cells utilize Toll-like receptor 7 [24, 25]. It is yet to be clarified which cells—hepatocytes or dendritic cells—have stronger potential to secrete IFN-λ at the single-cell level. However, it is rational to consider that serum IFN-λ_3 levels in patients are determined by the sum of IFN-λ_3 sporadically released from both types of cells. Therefore, it is plausible that the amount of IFN-λ released from hepatocytes or dendritic cells is influenced by the environment of the producers, such as inflammation and fibrosis. A positive correlation observed between serum IFN-λ_3 levels and AST levels, FIB-4 score, and APRI in B-CH patients may support such a possibility. In this study, serum IFN-λ_3 levels in the B-CH group were higher than those in HVs. However, this difference was slim compared with the difference between the C-CH group and HVs, suggesting that the difference in their genome structure, either RNA or DNA virus, may influence IFN-λ_3 production by infected cells. Of interest is the finding that serum IFN-λ_3 levels were higher in patients with acute hepatitis E than in patients with acute hepatitis A. It is reported that dendritic cells localized in the

Table 2 Correlation of interferon-λ_3 (*IFN-λ_3*) with clinical or immunological parameters in patients with chronic hepatitis C

Factors	CC with IFN-λ_3	*p*
Age (years)	−0.10	–
WBC (/mm^3)	−0.05	–
Hb (g/dL)	0.07	–
Plt ($\times 10^4$/mm^3)	−0.09	–
TP (g/dL)	0.07	–
Alb (g/dL)	−0.01	–
AST (U/L)	0.34	<0.0001
ALT (U/L)	0.34	<0.0001
T-bil (mg/dL)	0.03	–
T-chol (mg/dL)	−0.22	0.02
AFP (ng/mL)	0.30	0.001
HCV RNA (log IU/mL)	−0.05	–
Fibrosis score	0.07	–
Histological activity score	0.25	0.01
FIB-4 score	0.10	–
APRI	0.29	0.001
IP-10 (pg/mL)	0.53	<0.0001
MIP-1α (pg/mL)	−0.08	–
MIP-1β (pg/mL)	−0.18	–
RANTES (pg/mL)	0.26	–
PDGF-BB (pg/mL)	0.40	<0.0001

Alb albumin, *AFP* α-fetoprotein, *ALT* alanine aminotransferase, *APRI* aspartate aminotransferase platelet ratio index, *AST* aspartate aminotransferase, *CC* correlation coefficient by Spearman's analysis, *FIB-4* fibrosis-4, *Hb* hemoglobin, *HCV* hepatitis C virus, *IP-10* interferon-γ-inducible protein 10, *MIP-1α* macrophage inflammatory protein 1α, *MIP-1β* macrophage inflammatory protein 1β, *PDGF-BB* platelet-derived growth factor BB, *Plt* platelets, *RANTES* regulated on activation, normally T cell expressed, and secreted, *T-bil* total bilirubin, *T-chol* total cholesterol, *TP* total protein, *WBC* white blood cells

intestine are capable of producing IFN-λ in response to rotavirus to protect the host from infection [26]. Although both hepatitis E virus and hepatitis A virus are RNA viruses that are transmissible by the enterofecal route, the difference in serum IFN-λ_3 levels suggests that there are distinct mechanisms of recognition of hepatitis E virus and hepatitis A virus by the hosts. Further investigation is needed to disclose which pattern recognition receptors are utilized in hepatocytes or immune cells for the recognition of such viruses to produce IFN-λ.

The regulatory mechanisms of transcription and translation of IFN-λ_3 have not been well documented. The *IFNL3* SNPs (rs8099917) are located 8.9 kb upstream of the promoter region of the *IFNL3* gene [8, 9, 11]. Because of such localization, it is less likely that the genetic variation has some impact on the transcriptional level of *IFNL3*. With regard to the relationship between the *IFNL3* genotype and its transcripts, controversial results have been reported thus far. Some groups reported that IFN-λ_3 messenger RNA levels in peripheral blood mononuclear cells were higher in patients with the *IFNL3* major genotype than in those with the minor genotype [9]. In contrast, others showed that in hepatocytes such levels were comparable regardless of *IFNL3* SNPs. In the search for some genetic factors influencing *IFNL3* transcription, Sugiyama et al. [27] reported the existence of variable-length TA repeats in the promoter of the *IFNL3* gene. Other investigators showed that a certain structure of the 3′ untranslated region in the *IFNL3* gene is involved in the durability/stability of the gene [28]. Nevertheless, the contribution of such factors is not enough to fill in the gap, suggesting that certain other regulatory factors for *IFNL3* are still to be revealed.

Reports concerning serum IFN-λ in C-CH patients are limited. Langhans et al. [29] showed that serum levels of IFN-λ, which includes IFN-λ_2 and IFN-λ_3, were higher in patients with the *IFNL3* major genotype than in those with the minor genotype. One of the limitations of their study seems to be the lack of specificity for the measurement of IFN-λ_3. Since the homology of *IFNL2* (which encodes IFN-λ_2) and *IFNL3* is quite high, it is difficult to quantify specifically IFN-λ_3 by excluding contamination by IFN-λ_2. To exclude such a possibility, we used the newly developed chemiluminescence enzyme immunoassay for IFN-λ_3, which enables one to quantify IFN-λ_3 without any influence from IFN-λ_2 in the range from 0 to 1,000 pg/mL. By means of this system, we found that serum levels of IFN-λ_3 are not statistically different between patients with the *IFNL3* major genotype and those with the minor genotype.

On primary HCV exposure, the significance of IFN-λ family members as an antiviral protein is evident. However, such impact of IFN-λ_3 in chronically HCV-infected patients is still elusive. Langhans et al. [29] reported that serum IFN-λ levels in patients who had spontaneously cleared HCV were higher than in patients with chronic HCV infection, implying that a higher level of IFN-λ somewhat contributed to HCV eradication. In this study, we aimed to clarify the significance of IFN-λ_3 in patients with chronic HCV infection with different approaches. Firstly, we searched for the factors influencing serum IFN-λ_3 quantity by correlation analysis with clinical markers and multiple cytokines/chemokines. We found that AST, ALT, and α-fetoprotein levels and histological activity were positively correlated with serum IFN-λ_3 levels. In addition, one of the noninvasive fibrosis markers, APRI, was weakly correlated with serum IFN-λ_3 levels. Among the chemokines examined in this study, serum IFN-λ_3 was positively correlated with IP-10 and PDGF-BB. IP-10 (CXCL10) is induced in HCV-infected hepatocytes as one of the IFN-stimulated genes, and attracts CXCR3-positive T cells and natural killer cells and subsequently activates inflammation. IP-10 is also reported to be involved in the early stage of liver fibrosis [30, 31]. A similar fibrotic